Marine ecosystem changepoints spread under ocean warming in an Earth System Model

B. B. Cael[1], Charlotte Begouen Demeaux[1], Stephanie Henson[1], Charles A. Stock[2], Fernando Gonz´alez Taboada[2], Jasmin G. John[2], & Andrew D. Barton[3]

[1]National Oceanography Centre, Southampton, UK. [2]NOAA/OAR/Geophysical Fluid Dynamics Laboratory, New Jersey, USA. [3]Scripps Institution of Oceanography and Section of Ecology, Behavior and Evolution, University of California San Diego, La Jolla, CA, USA.

Marine ecosystem changepoints spread under ocean warming in an Earth System Model

B. B. Cael[1], Charlotte Begouen Demeaux[1], Stephanie Henson[1], Charles A. Stock[2], Fernando González Taboada[2], Jasmin G. John[2], & Andrew D. Barton[3]

[1]National Oceanography Centre, Southampton, UK.
[2]NOAA/OAR/Geophysical Fluid Dynamics Laboratory, New Jersey, USA.
[3]Scripps Institution of Oceanography and Section of Ecology, Behavior and Evolution, University of California San Diego, La Jolla, CA, USA

Key Points:

- Ocean area with changepoints in model plankton populations expands under anthropogenic climate change
- Hotspot regions where plankton changepoints occur frequently, corresponding to switches between alternate states, concurrently shrink
- Larger and/or heterotrophic plankton exhibit proportionally more changepoints

---

Corresponding author: B. B. Cael, `cael@noc.ac.uk`

Abstract

Sudden shifts in marine plankton communities in response to environmental changes are of special concern because of their low predictability and high potential impacts on ocean ecosystems. We explored how anthropogenic climate change influences the spatial extent and frequency of changepoints in plankton populations by comparing the behavior of a plankton community in a coupled Earth System Model under pre-industrial, historical 20th-century, and projected 21st-century forcing. The ocean areas where surface ocean temperature, nutrient concentrations, and different plankton types exhibited changepoints expanded over time. In contrast, regional hotspots where changepoints occur frequently largely disappeared. Heterotrophy and larger organism sizes were associated with more changepoints. In the pre-industrial and 20th century, plankton changepoints were associated with shifts in physical fronts, and more often with changepoints for iron and silicate than for nitrate and phosphate. In the 21st century, climate change disrupts these interannual-variability-driven changepoint patterns. Together, our results suggest anthropogenic climate change may drive less frequent but more widespread changepoints simultaneously affecting several components of pelagic food webs.

Plain Language Summary

Plankton are the backbone of pelagic ocean ecosystems and play important roles in regulating Earth's climate. Plankton populations and community structure respond to climate change, but much remains unknown about how climate change will influence plankton in the future. Here we look for rapid changes, or changepoints, in the virtual plankton communities of a global model simulating Earth's climate over the pre-industrial era, the 20th century, and a projection of 21st century climate change. We find, for all types of plankton in the model, that the ocean area where changepoints occur expands from the pre-industrial era into the 20th century and again from the 20th to the 21st century. At the same time, hotspot regions, where rapid changes occur at least a few times per century, tend to disappear for all plankton types, and for temperature. Large plankton are more susceptible to changepoints than small plankton, and zooplankton are more susceptible than phytoplankton. The model ecosystem response to climate change is complex and spatially variable, but suggests that rapid shifts in plankton communities may become increasingly widespread but less frequent as the climate warms.

1 Introduction

Phytoplankton and zooplankton comprise the lower trophic levels sustaining pelagic marine food webs, and play critical roles in global biogeochemical cycles, for example by fixing carbon and facilitating its export from the ocean surface (Falkowski et al., 1998; Stock et al., 2017; Sarmiento & Gruber, 2006). Plankton (i.e. phytoplankton and zooplankton) populations interact with numerous environmental factors, including most notably temperature, light, turbulence, pH, and nutrient concentrations (Margalef, 1978; Reynolds, 2006; Glibert, 2016; Kiorboe, 2008). Grazing by zooplankton provides an important constraint on phytoplankton population growth (Banse, 2013; Ward et al., 2012), and zooplankton themselves are subject to predation by higher trophic levels (Daewel et al., 2014). Plankton populations and their interactions respond to changes in environmental conditions, including both natural (Planque & Taylor, 1998; M. Edwards et al., 2013) and anthropogenic climate change (Bopp et al., 2013; Dutkiewicz et al., 2015; Barton et al., 2016). While such ecological changes can be gradual, there is substantial interest in cases where transitions to a new ecosystem state occur on a short time scale (here meaning closer to interannual than centennial timescales), because their downstream effects on carbon and nutrient cycling, fisheries, and other ecosystem services are intrinsically more difficult to adjust to or manage (deYoung et al., 2008; Conversi et al., 2015; Rocha et al., 2015).

Rapid changes in marine plankton populations may occur when changes in environmental conditions generate a sudden forcing on the community (Muller-Karger et al., 2019; Ardyna et al., 2014), or when gradual changes in environmental conditions provoke a nonlinear response (Scheffer et al., 2001; Stock et al., 2014a). With or without environmental forcing, rapid changes can also emerge from the internal dynamics of plankton communities (Di Lorenzo & Ohman, 2013; Barton et al., 2020; Huisman & Weissing, 1999). Because of the challenges of collecting long-term and broad-scale measurements of plankton populations (Benway et al., 2019), much remains unknown about how frequent abrupt changes are in the lower trophic levels of pelagic marine ecosystems, how abrupt changes differ with trophic status or organism size (Barton et al., 2020), how abrupt changes in plankton populations correspond to those in physical or chemical environmental conditions, or how their frequency and distribution will change (or already are changing) with climate change (Beaulieu et al., 2016).

Here we address these questions in the context of a plankton community model integrated into a global Earth System Model (ESM). The ESM includes a comprehensive ecosystem model, called Carbon, Ocean Biogeochemistry and Lower Trophics (COBALT), that captures regional and seasonal variations in integrated ecosystem properties (e.g. chlorophyll and primary production) as well as the emergent biogeographies of phytoplankton and zooplankton across contrasting body sizes, functional groupings, and predator-prey interactions (Stock & Dunne, 2010; Stock et al., 2014b). We investigate the occurrence of abrupt transitions in marine ecosystems through the analysis of changepoints, a general term defined as a time point where a change in a statistical property of a time series can be identified, but here more specifically meaning interannual, decadal, or multidecadal changes in trends or mean values (Reeves et al., 2007). We focused on centennial pre-industrial, historical, and projected climate change simulations for surface ocean temperature, nitrate concentrations, and phytoplankton and zooplankton of different sizes. Our objective is to map where changepoints occur and how frequent they are, with respect to oceanographic features, trophic levels, and climatic forcing. Our focus is specifically on plankton changepoints, and while it is unwieldy to establish the mechanisms underlying all individual plankton changepoints, we identify some common environmental drivers.

2 Materials and Methods

2.1 Numerical Model

Our analyses use simulations conducted with ESM2M-COBALT (Stock et al., 2014a). ESM2M-COBALT was derived from GFDL's ESM2M earth system model (Dunne et al., 2012, 2013) by replacing the ocean biogeochemical component with the Carbon, Ocean Biogeochemistry and Lower Trophics (COBALT, (Stock et al., 2014b)) model, while preserving other Earth system components. The ocean component is GFDL's Modular Ocean Model version 4.1 (MOM4p1) (Griffies, 2009) with a horizontal resolution of 1° and 50 vertical layers. The comprehensive ocean biogeochemistry and ecosystem COBALT model (Stock & Dunne, 2010; Stock et al., 2014a, 2014b) includes 33 prognostic tracers, including three phytoplankton groups, three zooplankton groups, and tracers representing the coupled elemental cycles of carbon, nitrogen, phosphorus, silicate, and iron, as well as alkalinity and lithogenic material. As described in Stock et al. (2014a), ESM2M-COBALT simulations follow the protocols of Phase 5 of the Coupled Model Intercomparison Project (CMIP5) (Flato et al., 2014) enlisted herein, and include 1) a 1500-year spinup simulation with 1860 radiative forcings and potential vegetation, the last 100 years of which are used as a pre-industrial (hereafter PI) control simulation, 2) a historical simulation from 1860-2004 featuring observed greenhouse gas concentrations, solar insolation, volcanic eruptions, ozone, and land use changes, from which we take the years 1901-2000 for the historical 20th century simulation, and 3) a future projection from (2) out to 2100 under the RCP8.5 scenario, the highest emission scenario among the set of Representative Concentration Pathway scenarios (Riahi et al., 2011), to which we append the years 2001-2004 from the historical simulation and hereafter refer to as the 21st century simulation (2001-2100). The ecological and biogeochemical properties from COBALT simulations compare well with global observations over the past few decades (Stock & Dunne, 2010; Stock et al., 2014a, 2014b, 2017).

Plankton traits and ecological interactions in the COBALT model are tied to body size (Stock et al., 2014a) and parametrized by allometric trait relationships gleaned from large compilations of laboratory measurements. For example, smaller model phytoplankton have higher nutrient affinity compared to the larger phytoplankton (K. F. Edwards et al., 2012), but are grazed upon by smaller, more efficient zooplankton (Hansen et al., 1997). Similar allometric trait formulations and trait-tradeoffs underpin other size-based plankton community models (Banas, 2011; Ward et al., 2012; Taniguchi et al., 2014; Baird & Suthers, 2007), and allow the COBALT model to plausibly simulate biogeographical and phenological patterns for a range of phytoplankton and zooplankton sizes (Stock et al., 2014b). Phytoplankton growth in the model is an increasing exponential function of temperature (Eppley, 1972), such that growth is higher at warmer temperatures and growth acclimates instantaneously to changes in temperature for each phytoplankton type. A similar Q_{10} was applied to zooplankton growth and grazing, although remineralization and particle aggregation and export were independent of temperature (Stock et al., 2014b). Plankton therefore do not have discrete temperature niches (Thomas et al., 2012)). In this study we use an identical model formulation to (Stock et al., 2014b). This type of size-structured plankton community model is ideal for studying how changepoints vary across body size and trophic level because it not only simulates these state variables but also because it encodes allometric gradients in physiological rates, generation times, and interaction strengths that are likely to influence the occurrence of model changepoints. For the purposes of our analyses, we exclude nitrogen-fixing phytoplankton (diazotrophs); while their presence in COBALT is essential for maintaining ocean surface nitrogen inventories, their traits and ecological interactions are not as well constrained as for other model phytoplankton (but see (Monteiro et al., 2011)) and their contribution to total productivity is modest. In our analyses, we use depth-integrated (over the top 100m) plankton biomass model output but temperature and nutrient data from the surface layer. We acknowledge that some changes could occur in depth distributions of plankton over the centuries of simulation that we do not resolve, but prefer instead to focus on horizontal and temporal patterns. The surface data for environmental properties are sufficient as we are interested in broad temporal and spatial gradients in these properties, rather than vertical profiles. Surface nutrients are used in conjunction with 100m-integrated biomass because surface nutrient values are most reflective of nutrient limitation in the euphotic zone.

The plankton community model in COBALT represents differences in body size and associated physiological traits and ecological interactions, as well as patterns of biogeography and phenology for model plankton types that are similar to observations (Stock et al., 2014b).

2.2 Changepoint Analysis

We then identify changepoints for the time series at each model grid box and in each simulation for each model variable of interest. In essence, changepoint methods are designed to identify points in a time series where a statistical property of that time series changes, such as its mean or its trend; such methods have been widely adopted by the statistics community for their robustness and ability to handle e.g. changes in time series with trends (Reeves et al., 2007; Killick et al., 2020). As we are analyzing the annually averaged output of centennial simulations, changepoints will necessarily be shifts between two multi-annual to multi-decadal average states, such as a switch between alternate stable states centered on different mean values, switches between increasing and

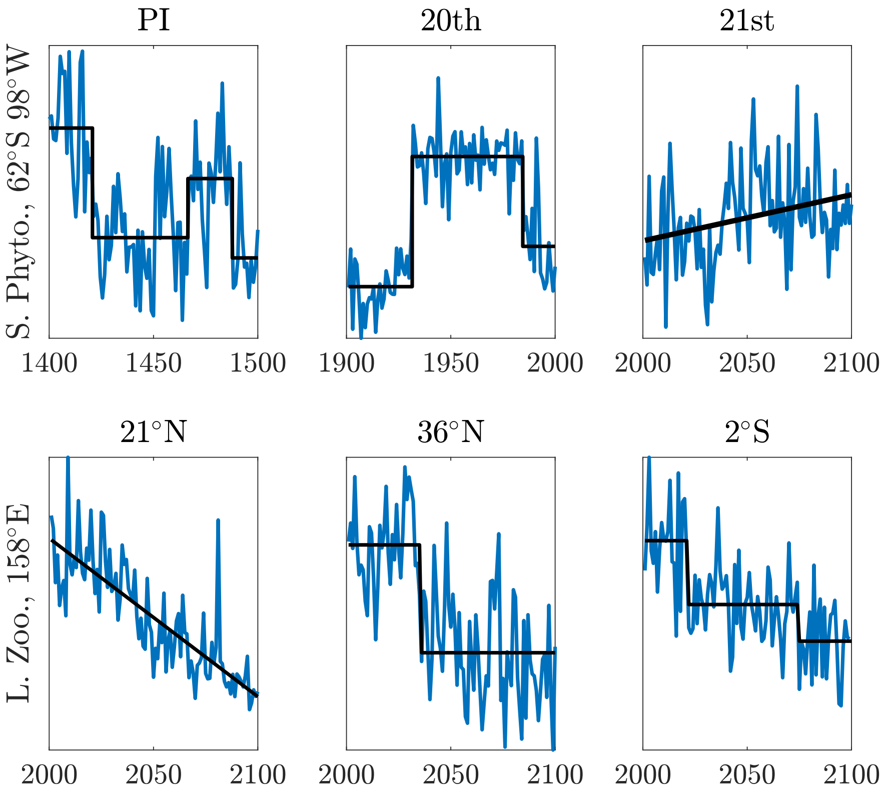

Figure 1. Example model small phytoplankton (top) time series at a single grid cell over different century simulations, and large zooplankton (bottom) time series at 158°E (where no changepoints occurred in the PI or 20th) in the 21st century (RCP8.5). At different centuries (top) or latitudes (bottom) either 0, 1, or 2 changepoints are identified.

decreasing trends, or the emergence of a multidecadal trend from a statistically steady baseline. We use the *EnvCpt* changepoint package in *R* (Killick et al., 2020), which relies on the Pruned Exact Linear Time algorithm (Killick et al., 2012) and selects among statistical models with changepoints relative to each other. We considered eight statistical models: 1) a constant mean, 2) a linear trend, 3) constant means with changepoints, 4) linear trends with changepoints, 5-8) AR(1) autoregressive versions of 1-4. We thus in essence fit each time series for each grid point, variable, and century simulation with a piecewise combination of constant values or linear trends, and formally define a changepoint as a point in a given time series where the best-fitting model switches between different segments of this piecewise fit. Qualitatively this corresponds to points in time where approximately interannual or (multi-)decadal shifts in the baseline value or baseline trend are identifiable. Figure S1 shows examples of each of these fit to COBALT time series, Figure 1 shows some example time series with different numbers of changepoints, and Table S1 shows a pedagogical example wherein the number of changepoints detected is robust to the superposition of a trend.

Both the presence and number of changepoints detected are robust across the models allowing abrupt changes (*i.e.* models 3, 4, 7 & 8 above detect the same number of changepoints for almost all grid cells for all three centuries). As we are interested in the quantitative characterization of the incidence and prevalence of changepoints, we group the statistical models into those with changepoints and those without, and hereafter focus on the absolute frequency of changepoints detected during each simulation, for each variable, and for each location. We also focus on this robust characteristic of the number of changepoints because the *EnvCpt* package does not require the piecewise linear models to be continuous; it also does not require changes to be of a certain amplitude for any statistical model. We discard all changepoints that occur in the first two or last two years of any time series to avoid edge effects. Note that the changepoint method does not require *ad hoc* parameters to be chosen, such as minimum segment length or transition magnitude. To report global changepoint statistics, we weight each grid cell proportional to its area. Note that we analyze each simulation separately. While the sign and occurrence of changepoints is a robust feature of our analysis, the quantification of the amplitude of a given changepoint depends on which of the eight aforementioned models is selected; because which model is selected as best-fitting is sensitive to the choice of fitting metric, we do not consider changepoint amplitude and instead focus on robust aspects of our analysis. In other words, all models 1-8 are fit to each variable, grid cell, and century time series to select the best-fitting model according to the Akaike Information Criterion. Then we focused on the number of changepoints detected by the selected model, which is a robust metric that is almost independent of model choice (i.e. using the Bayesian Information Criterion yields the same number of changepoints almost everywhere but different models). The overall incidence of changepoints may be more important than their specific magnitude, as recent work suggests that even small-amplitude ecological and biogeochemical changes can have appreciable consequences (Stock et al., 2014a; Barton et al., 2020).

3 Results and Discussion

The marine ecosystem model we employ exhibits a substantial increase in the prevalence (i.e. spatial extent) of changepoints during the 21st century under climate change conditions (RCP8.5), compared to historical 20th-century and pre-industrial era simulations (Figures 2, S2-10). We find fewer changepoints for smaller (phyto- and zoo-) plankton than larger plankton and fewer changepoints for phytoplankton than for zooplankton (§3.2), and that changepoints in plankton are more associated with iron and silicate than phosphate and nitrate, and more likely to occur where temporal shifts in latitudinal temperature gradients (a proxy for ocean fronts) are large (§3.3). However, the spatial extent of 'hotspot' locations, which have more frequent changepoints, reduces from the pre-industrial to the historical simulation and again from the historical to the future simulation (§3.4). (As we use the kurtosis of the probability distribution of the number of changepoints to quantify this, it is not specific to e.g. ≥ 3 or ≥ 4 changepoints per century. Here by hotspots we mean locations with ≥ 3 or ≥ 4 changepoints per century; the number chosen as the minimum per century does not affect our conclusions, but locations with ≥ 5 changepoints per year are very rare for some variables in some simulations.)

3.1 Spatiotemporal Changepoint Patterns

We first quantify and describe the spatial extent and distribution of changepoints in temperature, nutrient concentrations, and plankton populations across PI, 20th, and 21st century simulations (RCP8.5). In terms of changepoint spatial extent, four main features are apparent. The fraction of the upper ocean with changepoints increases for all variables only slightly from the PI to 20th century, but increases dramatically from the 20th to 21st century (Figures 2, 3, S2-10). Temperature has a smaller increase in changepoint extent between the 20th and 21st centuries than the other variables (Figure 3; the same is true to a lesser extent for iron). Nutrients other than iron have a much higher fraction of ocean area with changepoints that become widespread in the 21st century (>60% of ocean area affected) compared to the other variables. Finally, within each simulation the plankton populations show similar fractions of ocean area with changepoints, and the ranks are relatively stable across centuries and consistent with the scaling of generation time with body size (e.g. (Barton et al., 2020)). For example, small phytoplankton have changepoints in the smallest fraction of ocean area while large zooplankton have the largest fraction of ocean area with changepoints in each simulation. A plot of changepoint area for the 21st century (Figure 4) shows that the temporal distribution of these changepoints is somewhat uniform, with a peak in the 2060s (§3.5) and secondary peaks in the 2030s and 2010s.

In terms of spatial distributions, temperature changepoints are confined mostly to the high latitudes and Northeast Atlantic in the PI century, expanding equatorward in the 20th and 21st centuries (Figure S6). All the plankton exhibit variations of this pattern (Figures S2-5). Temperature changepoints in the PI and 20th centuries are primarily in Southern Ocean locations strongly influenced by interannual variability (Behrens et al., 2021; Auger et al., 2020). This region of the Southern Ocean has strong, approximately zonal fronts in sea surface height that create strong latitudinal gradients in temperature, nutrients, and ecosystems (Chapman et al., 2020). Observations from recent decades suggest that these fronts are moving poleward in response to climate change (Sallée et al., 2008; Sokolov & Rintoul, 2009; Kim & Orsi, 2014). The prevalence of changepoints in the Northeast Atlantic may be due to expansion and contraction of subtropical gyre extent (Polovina et al., 2008; Irwin & Oliver, 2009; Bograd et al., 2004) or variability in the wind-driven gyre circulation in this region, which is particularly variable through time (Häkkinen & Rhines, 2004; Hátún et al., 2005). Nitrate changepoints are, by contrast, concentrated in the subtropics in the PI and 20th centuries before becoming nearly global in the 21st century (RCP8.5; Figure S7). Nitrate changes primarily occur along the tropical fronts and in the subtropical gyres (associated with very different nutrient regimes) (Polovina et al., 2017), suggesting these fronts' interannual movements promote changepoints in upper ocean nitrate concentrations. Strong zonal fronts in environmental and ecological conditions that move meridionally on decadal to centennial timescales appear to be linked to changepoints in the model.

3.2 Trophic Changepoint Patterns

We also find an increase in the prevalence of changepoints from small to large phytoplankton, from small and medium to large zooplankton, and from phytoplankton to zooplankton, suggesting that changepoints are more widespread in larger organisms and higher tropic levels (Figure 5). Environmental variations are filtered through marine food webs, such that longer-lived organisms tend to exhibit more pronounced low frequency variability than do smaller, shorter-lived organisms (Di Lorenzo & Ohman, 2013; Barton et al., 2020). In other words, the greater area of changepoints in larger organisms and higher trophic levels may be caused, in part, by intrinsic trophic amplification within food webs (Stock et al., 2014a; Chust et al., 2014), which exacerbates extrinsic environmental and climate forcing.

3.3 Drivers of Plankton Changepoints

Plankton changepoints in the PI and 20th century can be understood as switches between alternate states associated with movements of frontal positions and co-located shifts with certain nutrients. These relationships break down in the 21st century as these sorts of changepoints are likely eclipsed by the emergence of climate-change-driven trends that appear to emerge differently for different variables and suppress pre-existing patterns of variability (either entirely or to the point of statistical insignificance). In the PI and 20th century, we see that the correlations of different plankton changepoints' locations with each other are fairly strong (Figure 6).

Spatial correlations in the frequency of changepoints here capture whether changepoints occur in each variable at the same frequency and in the same locations. In other

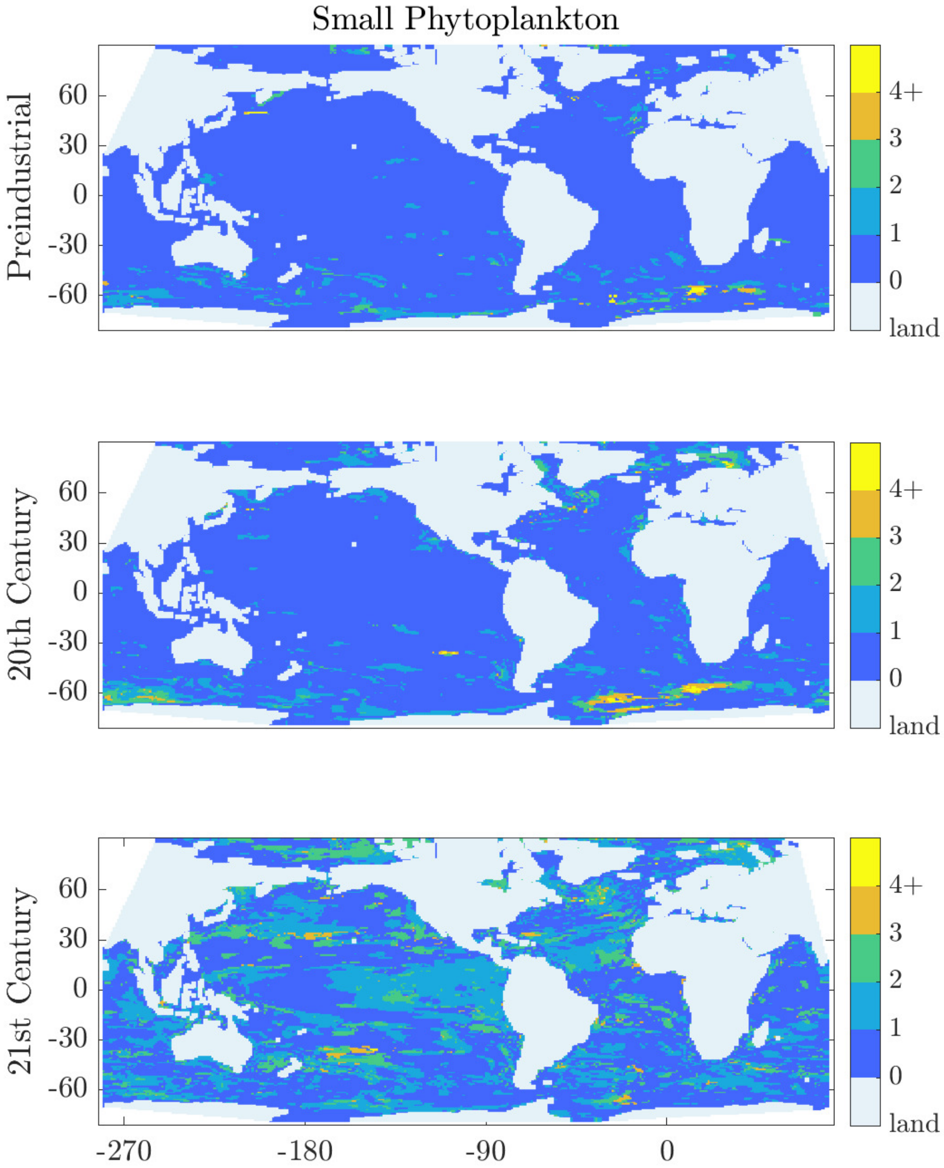

Figure 2. Maps of number of changepoints for each simulation for small phytoplankton. See Figures S2-10 for other plankton, temperature, and nutrients.

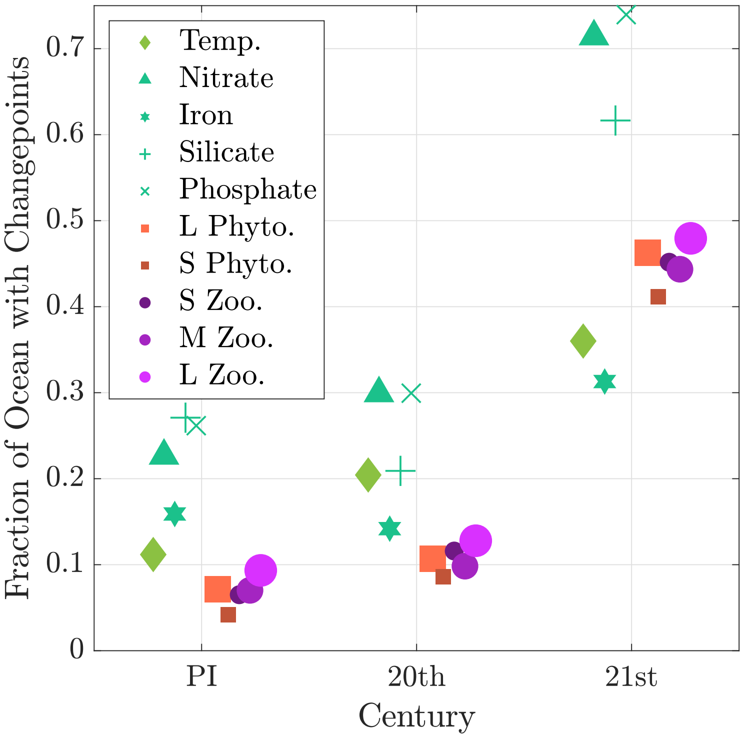

Figure 3. Fraction of ocean area with changepoints for each variable and simulation (calculated by summing up the total ocean area with at least one changepoint and dividing by the total ocean area). Points are offset from each vertical line as a visual aide.

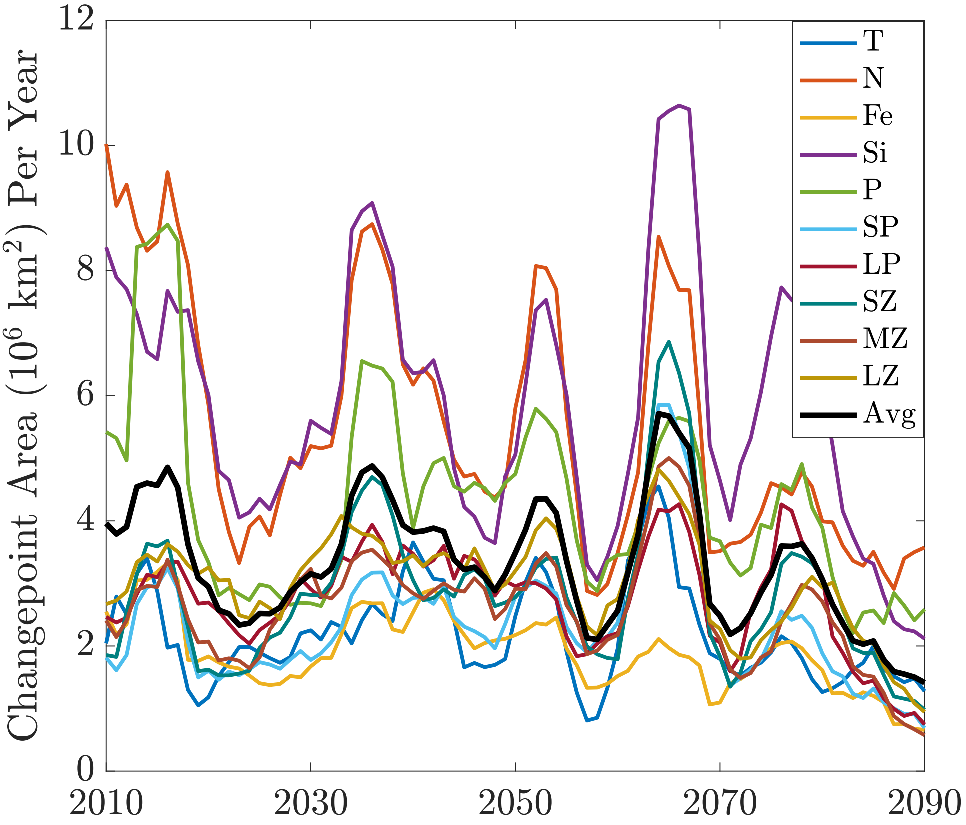

Figure 4. Area exhibiting a changepoint in each variable for each year in the climate change simulation. The legend refers respectively to temperature, nitrate, iron, silicate, phosphate, small and large phytoplankton, small, medium and large zooplankton, and the average of all ten of these. Data have been smoothed with a 5-year running mean for visual clarity. Changepoints in the first and last decade of each century have been excluded from this figure as these are more liable to be due to edge effects (Killick et al., 2012).

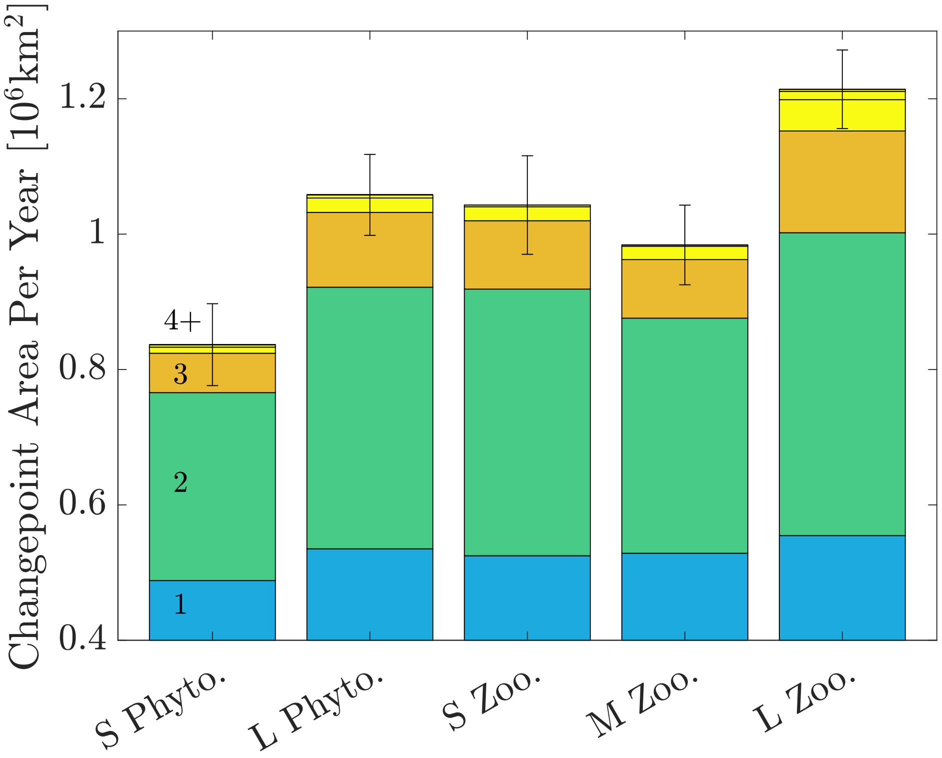

Figure 5. Barplot of area where changepoints occur for each plankton variable over all three simulations. Bars are split (by color) by contribution from grid cells with different total number of changepoints across the simulations. Error bars correspond to decadal variability (standard deviation of decadal averages) in the mean changepoint area per year.

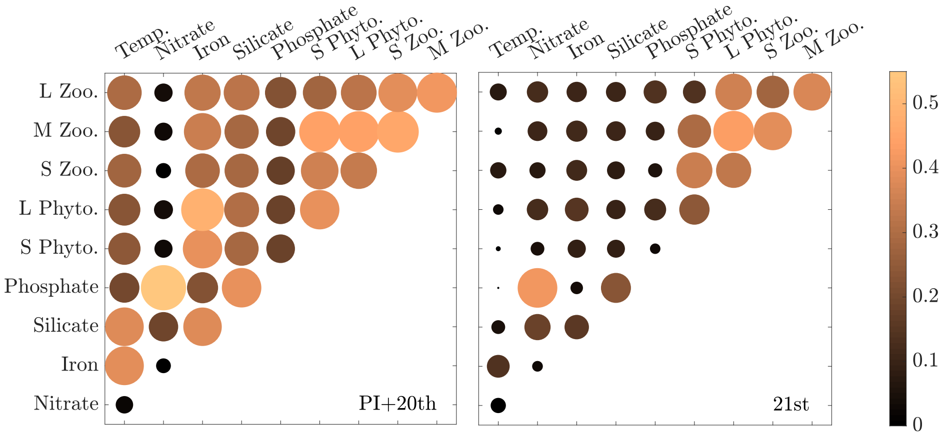

Figure 6. Correlations between the locations of changepoints of each variable in the PI and 20th century simulations (left) and the 21st century simulation. Circle size and color both correspond to correlation magnitude (see text for definition). Changes between PI and 20th century simulations (left) and the 21st century simulation for all correlations (except nitrate-phosphate, nitrate-small zooplankton, and small zooplankton-medium zooplankton) are significant ($p < 0.01$).

words, the correlation ρ_{ij} of variable i with variable j is calculated by defining a vector for both variables N_k^i and N_k^j of the number of changepoints that occur at each grid point k for that variable, and then computing the weighted Pearson correlation for those vectors, weighted by the area of each grid point k. This is preferred to a simple binary association such as a phi coefficient (Cramir, 1946) because variables can have multiple changepoints at a single location across a given time series.

In terms of nutrients, we find that plankton changepoints are most strongly correlated with changepoints in iron, then silicate, then phosphate, then least of all nitrate (Figure 6). Correlations with temperature changepoints are moderate (Figure 6). These correlations between e.g. iron and plankton changepoint locations in the PI and 20th centuries suggest that an appreciable fraction of these plankton changepoints reflect changepoints in these environmental variables, or alternatively similar phenomena specific to these locations are driving changepoints in correlated variables. These correlations also suggest that nitrate's changepoint dynamics are quite different than those for the other variables, because the locations of nitrate changepoints are only very weakly correlated with those of other variables across all simulations. This may in part be due to the greater complexity of the nitrogen cycle than that of other nutrients.

We also find that changepoints in the PI and 20th century tend to be associated with switches between alternate states; Figure 7 shows that in these centuries, most consecutive changepoints at a given location disagree in sign, i.e. if one changepoint is associated with a increase in a baseline concentration or trend, the subsequent changepoint is usually associated with a decrease in that baseline concentration or trend. This may be because changepoints in the PI and 20th centuries are strongly associated with shifts in the position of ocean fronts, which meander on interannual to multidecadal timescales. Figure 8 shows the frequency of changepoints, for a given century and variable, as a function of the temporal change in the latitudinal temperature gradient, $\partial|\partial T/\partial y|/\partial t$. Large latitudinal temperature gradients $|\partial T/\partial y|$ are commonly a proxy for the positions of ocean

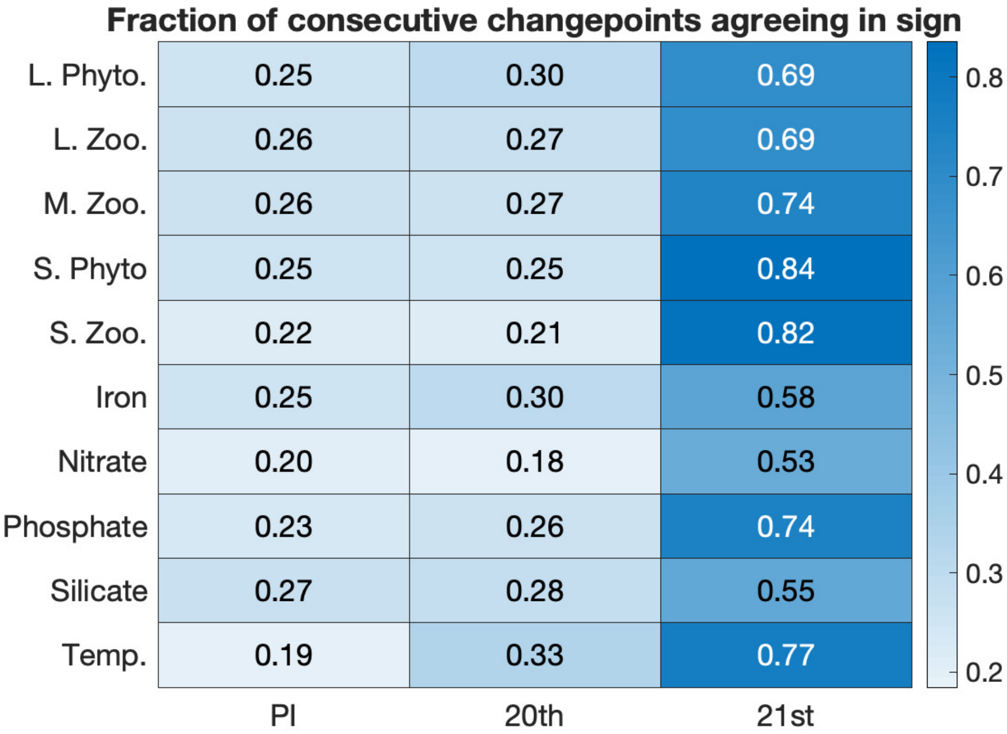

	PI	20th	21st
L. Phyto.	0.25	0.30	0.69
L. Zoo.	0.26	0.27	0.69
M. Zoo.	0.26	0.27	0.74
S. Phyto	0.25	0.25	0.84
S. Zoo.	0.22	0.21	0.82
Iron	0.25	0.30	0.58
Nitrate	0.20	0.18	0.53
Phosphate	0.23	0.26	0.74
Silicate	0.27	0.28	0.55
Temp.	0.19	0.33	0.77

Figure 7. Fraction of consecutive changepoints at the same location that have the same sign, for each variable and century. Colors and numbers in squares indicate fraction.

fronts; temporal changes in these are then indicative of changes in frontal positions over time. (We evaluated this for decadally averaged temperature values because the model's latitudinal temperature gradients are noisy on annual timescales.) For a given variable and century, a relative probability of changepoint occurrence of, for example, 2 for a given value of $\partial|\partial T/\partial y|/\partial t$, e.g. 0.05 °C/°N/decade, means that changepoints are twice as likely to occur, relative to the global average, at places and times when $\partial|\partial T/\partial y|/\partial t =$ 0.05 °C/°N/decade. The strong increase in this relative probability with $\partial|\partial T/\partial y|/\partial t$ in the PI and 20th century for all plankton variables, temperature, silicate, and iron indicates that changepoints in these centuries and variables are associated with shifts in frontal positions.

In the 21st century, however, the correlations between plankton changepoints' locations and those of the environmental variables all decrease to near zero (Figure 6), the association between temporal changes in frontal positions all but disappear (Figure 8), and the sign-disagreement of consecutive changepoints is reversed such that consecutive changepoints tend to be reinforcing in most cases (Figure 7). Altogether this underscores that changepoints in the 21st century are of a qualitatively different nature than those of the PI and 20th century, neither due to changes in frontal positions nor switching between alternate states. This indicates that climate-change-driven changepoints disrupt pre-existing interannual-variability-driven changepoint patterns of plankton ecosystems, raising the question of how best to describe plankton changepoint patterns in the future if patterns of variability are distinct from the past. Furthermore the lack of co-location in our model of plankton and nutrient changepoints draws into question the extent that nutrients may be indicators of multidecadal changes in plankton ecosystems.

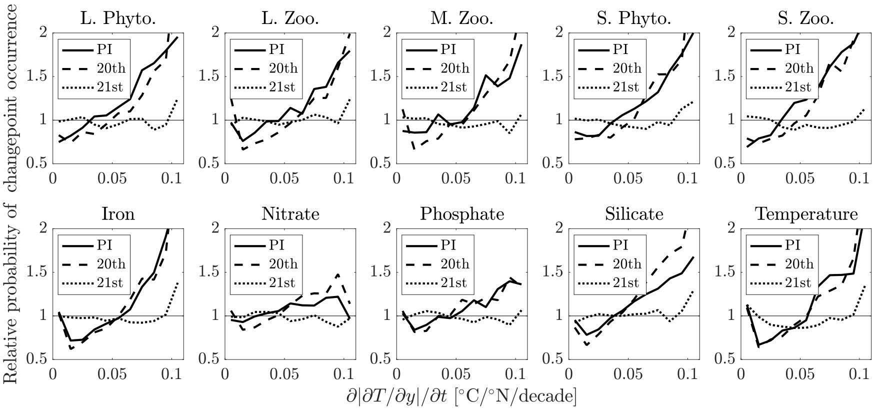

Figure 8. The relative frequency of changepoints occurring in places and times with different values of shifts in latitudinal temperature gradients, for each variable and century simulation.

3.4 Changepoint Hotspots

In addition to quantifying which locations experience and do not experience ecological changepoints in which variables, we also consider how frequent changepoints are in locations that have them. While the average numbers of plankton changepoints per century (in locations where there are changepoints) remains fairly stable (Figure S11), more surprisingly we found that plankton (and temperature) changepoint 'hotspots' (locations with ≥3 or ≥4 changepoints per century) tend to disappear over time. In other words, in places where changepoints are frequent, the rate at which changepoints occur slows down. This is most simply quantified by the excess kurtosis ($\kappa = \mu_4/\sigma^4 - 5.99$, where $\mu_4(X) = E[(X - \mu)^4)]$ is the fourth central moment and σ is the standard deviation) of the changepoint distribution, where 5.99 is used instead of the usual value of 3 because the number of changepoints is non-negative; 5.99 is the kurtosis of an integer-rounded half-normal distribution (Figure S12). The kurtosis is a standard measure of a distribution's heavy-tailed-ness; a positive κ indicates that the distribution has a heavier tail than an integer-rounded half-normal, and the larger the κ, the heavier the tail. In this context, a heavy tail means that changepoints tend to be concentrated in 'hotspot' locations where changepoints occur frequently (Figures S12, S13). Note that the kurtosis κ is only a measure of the probability distribution of the number of changepoints and is therefore not affected by the total ocean area experiencing changepoints or the total number of changepoints. Figure S13 also shows the changepoint probability distribution for small phytoplankton for each century to illustrate what a smaller excess kurtosis means in terms of the disappearance of changepoint hotspots.

Figure 9 shows the excess kurtosis κ for each variable and simulation. While all variables besides nitrate are somewhat heavy-tailed in the PI century, the most heavy-tailed being small and large zooplankton, we find a decline in excess kurtoses across the plankton types (and for temperature) in the 20th and 21st centuries (RCP8.5). This demonstrates the disappearance of changepoint hotspots for all plankton (and for temperature), even after accounting for the increase in ocean area experiencing changepoints (Figures 3, S14). Changepoint hotspots for large and medium zooplankton, and large phytoplankton mostly disappear in the 20th century, whereas small phytoplankton and zooplankton and temperature show declines between both the PI and 20th centuries and between the 20th and 21st centuries. Note that this is not driven by an increase in the area with a low number of changepoints, i.e. locations switching from having no changepoints to having low numbers of changepoints over time, because 1) the means of these distributions do not change substantially or consistently over time (Figure S11), 2) the total area

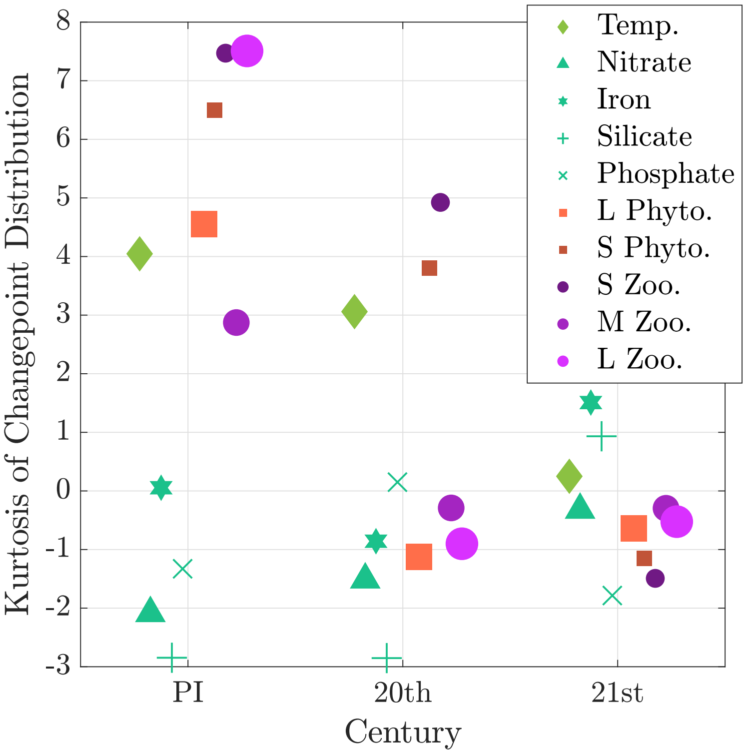

Figure 9. Excess kurtosis of the distribution of the number of changepoints per unit area per century for each variable. High values of excess kurtosis indicate spatial clustering of changepoints into 'hotspots'. Figure S12 shows how a reduction in kurtosis corresponds to a reduction in a distribution's tail; Figure S13 shows an example of a changepoint distribution's change across simulations; Figure S14 shows that the decrease in kurtosis seen here holds when only considering locations with changepoints in the PI and/or 20th century simulations for each variable.

of locations with 4+ changepoints also decreases with time for all plankton (from between 0.88-2.4% in the PI century to between 0.08-0.87% in the 21st century; Figures 2, S2-10), and 3) this decrease in excess kurtosis also holds when restricting only to locations that have changepoints in the PI or 20th century (Figure S14).

For plankton and temperature, these hotspots all occur in the polar oceans and in the northeast Atlantic (though different variables' hotspots are not always perfectly co-located). Hotspots likely disappear with climate forcing because plankton communities that were previously switching frequently between alternative states no longer do so in the novel environmental conditions into which they are pushed. Temperature changepoint hotspots, concentrated in the high latitudes in the PI and 20th centuries, likely vanish with the poleward recession of seasonal sea ice in the 21st century out of latitudes where temperature has sufficient interannual variability. Nutrients are the exception in Figure 9, with κ values near zero or negative in the PI and 20th centuries, indicating a comparative absence of hotspots. Changes across centuries in nutrients' κ values are smaller, increasing slightly overall from PI to the 21st century. The lack of systematic or substantial change in nutrients' κ values likely reflects that these hotspots' shifts are not eclipsed by climate-change-driven trends. Plankton populations draw nutrient concentrations down to subsistence concentrations, and therefore nutrient concentrations should have a threshold-like behavior (Tilman, 1982). Food web adjustments that stabilize changes in nutrients

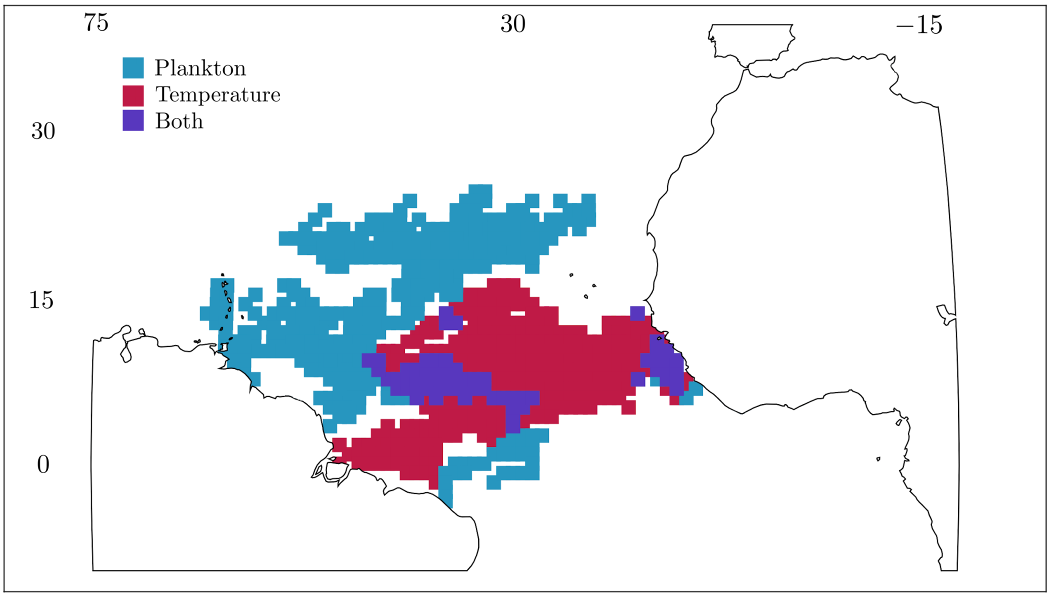

Figure 10. Changepoints in the subtropical North Atlantic in the 2060s under RCP8.5. Red indicates where changepoints in temperature occur in 2063. Blue indicates where changepoints in the biomass of one or more plankton occur in 2065 and 2066. Purple indicates changepoint in both. Small changepoint areas (<10 contiguous grid cells) are not plotted. Latitude is in degrees North, and longitude is in degrees west.

may be too small to be identified as changepoints, such that nutrients retain their changepoint hotspots despite climate-change-driven shifts but plankton do not.

3.5 Illustrative Example of a Large-scale Ecological Shift

To illustrate the emergence and propagation of extensive changepoints during the 21st century simulation, we show here a temperature driven shift affecting the tropical Atlantic. Temperature is included not only as a driver of plankton dynamics via affecting metabolic and interaction rates and local water column dynamics, but also as a reflection of changes in ocean and atmospheric physics. A changepoint in temperature can indicate an adjustment of the coupled ocean-atmosphere physical system, for instance in response to external forcing. Temperature changepoints may bring about subsequent changepoints in other variables that are not necessarily co-located, as captured by Figure 6. We find possible evidence of this in our 21st century simulation (RCP8.5) of the GFDL COBALT model. In year 2063, we find a large, coherent area with changepoints in temperature in the equatorial North Atlantic (Figure 10). This one contiguous changepoint region subsumes 50% of the global area where temperature has a changepoint in 2063 and results in a far larger total area experiencing a changepoint in temperature in 2063 than in any other model year (Figure 4). Subsequently, in years 2065 and 2066, a large adjacent area of changepoints occurs in model plankton (Figure 10). The number of plankton changepoints in this region during these years exceeds any other two-year model period.

These maxima are attributable to a large contiguous region northwest of the 2063 temperature changepoint region where plankton populations have changepoints in 2065 and 2066 (Figure 10). A coherent changepoint region in temperature in 2063 could be due to a large-scale adjustment of the ocean-atmosphere physical system, with large-scale ecological effects in the following few years. That no nutrient shows corresponding changepoints in the low-latitude Atlantic Ocean at this time suggests this is the direct influence of temperature and/or circulation on the plankton populations. The location of two changepoint regions suggests that this effect may be an adjustment of the North Atlantic Overturning Circulation, which is expected to shift with climate change, potentially abruptly (Buckley & Marshall, 2016). Note that this result should be taken as an illustrative example of this possibility and that future studies should carefully diagnose on a location by location basis how ocean and atmosphere circulation can promote change points in ocean environment and plankton.

4 Conclusion

We explored the spatial distribution and frequency of changepoints in a plankton community model within an Earth System Model over three centennial simulations representing the pre-industrial period (the final 100 years of a 1500 year control simulation), 20th century (1901-2000), and climate warming conditions in the 21st century (RCP8.5, 2001-2100). Anthropogenic forcing in the 21st century results in a substantial increase of ocean area where plankton abundances have changepoints, relative to the preindustrial era and 20th century. However, changepoint hotspots in the Southern Ocean and Northeast Atlantic Ocean, where plankton concentrations or temperature frequently undergo changepoints, largely disappear from the preindustrial period to the 21st century, as plankton communities that were previously switching frequently between alternative states no longer do so in the novel environmental conditions into which they are pushed. In agreement with the hypothesis of trophic amplification, larger plankton have more changepoints than smaller plankton, and zooplankton have more changepoints than phytoplankton; changepoints also often propagate through pelagic food webs rather than being restricted to individual plankton types. Plankton changepoints in the preindustrial and 20th centuries are associated with changes in frontal positions, certain nutrients (especially iron and least of all nitrate), and switches between alternate states. None of this is the case in the 21st century, when instead climate-change-driven changepoints disrupt pre-existing interannual-variability-driven changepoint patterns of plankton ecosystems. Temperature changepoints may reflect ocean-atmosphere physics changes with nonlocal effects, as illustrated by a large changepoint region in the equatorial North Atlantic in model year 2063 preceding a large plankton changepoint region to its northwest in years 2065 and 2066. These results suggest that globally, plankton populations are susceptible to abrupt changes as a result of anthropogenic climate change, and that population dynamics are important for such changes, with larger organisms and higher trophic levels being more susceptible.

We note though that while latitudinal temperature gradients and nutrient concentrations are critical drivers of plankton communities, they are only some of many environmental factors that influence them; rapid plankton community responses associated with gradual warming may still reflect rapid changes in other environmental factors. We also emphasize that we have only considered one Earth system model here, and our results are specific to this model and likely differ in particular patterns if not mechanisms for other models. It would be instructive to test whether similar results and mechanism underlying changepoints hold for other ecosystem models, and even more so whether complex ecosystem models that are able to predict properties such as phytoplankton diversity show similar results, and how these ecosystem properties are projected to change in the future. As the propensity for rapid ecological changes may either increase or decrease with system complexity (McCann, 2000), investigating the susceptibility of model populations to rapid changes across a range of ecosystem complexities will be essential to assessing the implications of model results for marine ecosystems (Cael et al., 2021). The approach we use here may also be suitable for terrestrial systems as well, particularly when considering differences in changepoint extent and frequency across organism size and trophic level at regional and larger spatial scales.

Acknowledgments

We thank John Dunne for providing an internal GFDL review of a previous version of this manuscript, four anonymous reviewers for helpful comments on a previous version of this manuscript, and Claudie Beaulieu for helpful advice on the correction application of the envcpt R package.

BBC and SH acknowledge support from the National Environmental Research Council (NE/R015953/1). BBC and SH have also received funding from the European Union's Horizon 2020 Research and Innovation Programme under grant agreement No. 820989 (project COMFORT, our common future ocean in the Earth system – quantifying coupled cycles of carbon, oxygen, and nutrients for determining and achieving safe operating spaces with respect to tipping points).

The work reflects only the authors' view; the European Commission and their executive agency are not responsible for any use that may be made of the information the work contains. The model outputs used here are in the process of being archived and will be available at [Zenodo DOI] by the time of acceptance should the manuscript be accepted for publication. In the meantime, reviewers can access them at the GFDL FTP site (ftp.gfdl.noaa.gov, login: anonymous, password: e-mail address) at /pub/Charles.Stock/Caeletal_GRL_Submission.

References

Ardyna, M., Babin, M., Gosselin, M., Devred, E., Rainville, L., & Tremblay, J.-É. (2014). Recent arctic ocean sea ice loss triggers novel fall phytoplankton blooms. *Geophysical Research Letters*, *41*(17), 6207–6212.

Auger, M., Morrow, R., Kestenare, E., & Sallée, J.-B. (2020). Southern ocean in-situ temperature trends over 25 years emerge from interannual variability.

Baird, M. E., & Suthers, I. M. (2007). A size-resolved pelagic ecosystem model. *Ecological Modelling*, *203*(3-4), 185–203.

Banas, N. S. (2011). Adding complex trophic interactions to a size-spectral plankton model: emergent diversity patterns and limits on predictability. *Ecological modelling*, *222*(15), 2663–2675.

Banse, K. (2013). Reflections about chance in my career, and on the top-down regulated world. *Annual Review of Marine Science*, *5*(1), 1–19. doi: 10.1146/annurev-marine-121211-172359

Barton, A. D., Irwin, A. J., Finkel, Z. V., & Stock, C. A. (2016). Anthropogenic climate change drives shift and shuffle in north atlantic phytoplankton communities. *Proceedings of the National Academy of Sciences*, *113*(11), 2964–2969.

Barton, A. D., Taboada, F. G., Atkinson, A., Widdicombe, C. E., & Stock, C. A. (2020). Integration of temporal environmental variation by the marine plankton community. *Marine Ecology Progress Series*, *647*, 1–16.

Beaulieu, C., Cole, H., Henson, S., Yool, A., Anderson, T., De Mora, L., … Allen, J. (2016). Marine regime shifts in ocean biogeochemical models: a case study in the gulf of alaska. *Biogeosciences*, *13*(15), 4533–4553.

Behrens, E., Hogg, A. M., England, M. H., & Bostock, H. (2021). Seasonal and interannual variability of the subtropical front in the new zealand region. *Journal of Geophysical Research: Oceans*, *126*(2), e2020JC016412.

Benway, H. M., Lorenzoni, L., White, A. E., Fiedler, B., Levine, N. M., Nicholson, D. P., … others (2019). Ocean time series observations of changing marine ecosystems: an era of integration, synthesis, and societal applications. *Frontiers in Marine Science*. doi: https://doi.org/10.3389/fmars.2019.00393

Bograd, S. J., Foley, D. G., Schwing, F. B., Wilson, C., Laurs, R. M., Polovina, J. J., . . . Brainard, R. E. (2004). On the seasonal and interannual migrations of the transition zone chlorophyll front. *Geophysical Research Letters*, *31*(17).

Bopp, L., Resplandy, L., Orr, J. C., Doney, S. C., Dunne, J. P., Gehlen, M., . . . others (2013). Multiple stressors of ocean ecosystems in the 21st century: projections with cmip5 models. *Biogeosciences*, *10*, 6225–6245.

Buckley, M. W., & Marshall, J. (2016). Observations, inferences, and mechanisms of the atlantic meridional overturning circulation: A review. *Reviews of Geophysics*, *54*(1), 5–63.

Cael, B., Dutkiewicz, S., & Henson, S. (2021). Abrupt shifts in 21st-century plankton communities. *Science advances*, *7*(44), eabf8593.

Chapman, C. C., Lea, M.-A., Meyer, A., Sallée, J.-B., & Hindell, M. (2020). Defining southern ocean fronts and their influence on biological and physical processes in a changing climate. *Nature Climate Change*, *10*(3), 209–219.

Chust, G., Allen, J. I., Bopp, L., Schrum, C., Holt, J., Tsiaras, K., . . . others (2014). Biomass changes and trophic amplification of plankton in a warmer ocean. *Global Change Biology*, *20*(7), 2124–2139.

Conversi, A., Dakos, V., Gårdmark, A., Ling, S., Folke, C., Mumby, P. J., . . . Mollmann, C. (2015). A holistic view of marine regime shifts. *Philosophical Transactions of the Royal Society B*, *370*, 20130279. doi: 10.1098/rstb.2013.0279

Cramir, H. (1946). Mathematical methods of statistics. *Princeton U. Press, Princeton*, *500*.

Daewel, U., Hjøllo, S. S., Huret, M., Ji, R., Maar, M., Niiranen, S., . . . van de Wolfshaar, K. E. (2014). Predation control of zooplankton dynamics: a review of observations and models. *ICES Journal of Marine Science*, *71*(2), 254–271.

deYoung, B., Barange, M., Beaugrand, G., Harris, R., Perry, R. I., Scheffer, M., & Werner, F. (2008). Regime shifts in marine ecosystems: detection, prediction and management. *Trends in Ecology and Evolution*, *27*(3), 402–409. doi: 10.1016/j.tree.2008.03.008

Di Lorenzo, E., & Ohman, M. D. (2013). A double-integration hypothesis to explain ocean ecosystem response to climate forcing. *Proceedings of the National Academy of Sciences*, *110*(7), 2496–2499.

Dunne, J. P., John, J. G., Adcroft, A. J., Griffies, S. M., Hallberg, R. W., Shevliakova, E., . . . others (2012). Gfdl's esm2 global coupled climate–carbon earth system models. part i: Physical formulation and baseline simulation characteristics. *Journal of climate*, *25*(19), 6646–6665.

Dunne, J. P., John, J. G., Shevliakova, E., Stouffer, R. J., Krasting, J. P., Malyshev, S. L., . . . others (2013). Gfdl's esm2 global coupled climate–carbon earth system models. part ii: carbon system formulation and baseline simulation characteristics. *Journal of Climate*, *26*(7), 2247–2267.

Dutkiewicz, S., Morris, J. J., Follows, M. J., Scott, J., Levitan, O., Dyhrman, S. T., & Berman-Frank, I. (2015). Impact of ocean acidification on the structure of future phytoplankton communities. *Nature Climate Change*, *5*(11), 1002–1006.

Edwards, K. F., Thomas, M. K., Klausmeier, C. A., & Litchman, E. (2012). Allometric scaling and taxonomic variation in nutrient utilization traits and maximum growth rate of phytoplankton. *Limnology and Oceanography*, *57*(2), 554–566.

Edwards, M., Beaugrand, G., Helaouët, P., Alheit, J., & Coombs, S. (2013). Marine ecosystem response to the atlantic multidecadal oscillation. *PloS one*, *8*(2), e57212.

Eppley, R. W. (1972). Temperature and phytoplankton growth in the sea. *Fish. bull*, *70*(4), 1063–1085.

Falkowski, P. G., Barber, R. T., & Smetacek, V. (1998). Biogeochemical controls and feedbacks on ocean primary production. *Science*, *281*, 200–206. doi: 10

.1126/science.281.5374.200

Flato, G., Marotzke, J., Abiodun, B., Braconnot, P., Chou, S. C., Collins, W., . . . others (2014). Evaluation of climate models. In *Climate change 2013: the physical science basis. contribution of working group i to the fifth assessment report of the intergovernmental panel on climate change* (pp. 741–866). Cambridge University Press.

Glibert, P. M. (2016). Margalef revisited: A new phytoplankton mandala incorporating twelve dimensions, including nutritional physiology. *Harmful Algae*, *55*, 25–30. doi: 10.1016/j.hal.2016.01.008

Griffies, S. (2009). *Elements of mom4p1. noaa/geophysical fluid dynamics laboratory.* Princeton.

Häkkinen, S., & Rhines, P. B. (2004). Decline of subpolar north atlantic circulation during the 1990s. *Science*, *304*(5670), 555–559.

Hansen, P. J., Bjørnsen, P. K., & Hansen, B. W. (1997). Zooplankton grazing and growth: Scaling within the 2-2,-μm body size range. *Limnology and oceanography*, *42*(4), 687–704.

Hátún, H., Sandø, A. B., Drange, H., Hansen, B., & Valdimarsson, H. (2005). Influence of the atlantic subpolar gyre on the thermohaline circulation. *Science*, *309*(5742), 1841–1844.

Huisman, J., & Weissing, F. J. (1999). Biodiversity of plankton by species oscillations and chaos. *Nature*, *402*(6760), 407–410.

Irwin, A. J., & Oliver, M. J. (2009). Are ocean deserts getting larger? *Geophysical Research Letters*, *36*(18).

Killick, R., Beaulieu, C., Taylor, S., & Hullait, H. (2020). EnvCpt: Detection of Structural Changes in Climate and Environment Time Series [Computer software manual]. Retrieved from `https://CRAN.R-project.org/package=EnvCpt` (R package version 1.1.2)

Killick, R., Fearnhead, P., & Eckley, I. A. (2012). Optimal detection of changepoints with a linear computational cost. *Journal of the American Statistical Association*, *107*(500), 1590–1598.

Kim, Y. S., & Orsi, A. H. (2014). On the variability of antarctic circumpolar current fronts inferred from 1992–2011 altimetry. *Journal of Physical Oceanography*, *44*(12), 3054–3071.

Kiorboe, T. (2008). *A mechanistic approach to plankton ecology.* Princeton University Press. doi: 10.1515/9780691190310

Margalef, R. (1978). Life'forms of phytoplankton as survival alternatives in an unstable environment. *Oceanologica Acta*, *1*(4), 493–509.

McCann, K. S. (2000). The diversity–stability debate. *Nature*, *405*(6783), 228–233.

Monteiro, F. M., Dutkiewicz, S., & Follows, M. J. (2011). Biogeographical controls on the marine nitrogen fixers. *Global Biogeochemical Cycles*, *25*(2).

Muller-Karger, F. E., Astor, Y. M., Benitez-Nelson, C. R., Buck, K. N., Fanning, K. A., Lorenzoni, L., . . . others (2019). The scientific legacy of the cariaco ocean time-series program. *Annual Review of Marine Science*, *11*, 413–437.

Planque, B., & Taylor, A. H. (1998). Long-term changes in zooplankton and the climate of the north atlantic. *ICES Journal of Marine Science*, *55*(4), 644–654.

Polovina, J. J., Howell, E. A., & Abecassis, M. (2008). Ocean's least productive waters are expanding. *Geophysical Research Letters*, *35*(3).

Polovina, J. J., Howell, E. A., Kobayashi, D. R., & Seki, M. P. (2017). The transition zone chlorophyll front updated: advances from a decade of research. *Progress in Oceanography*, *150*, 79–85.

Reeves, J., Chen, J., Wang, X. L., Lund, R., & Lu, Q. Q. (2007). A review and comparison of changepoint detection techniques for climate data. *Journal of applied meteorology and climatology*, *46*(6), 900–915.

Reynolds, C. S. (2006). *Ecology of Phytoplankton.* New York, NY, USA: Cambridge University Press.

Riahi, K., Krey, V., Rao, S., Chirkov, V., Fischer, G., Kolp, P., … Rafai, P. (2011). Rcp-8.5: exploring the consequence of high emission trajectories. *Climatic Change. doi*, *10*, 1007.

Rocha, J., Yletyinen, J., Biggs, R., Blenckner, T., & Peterson, G. (2015). Marine regime shifts: drivers and impacts on ecosystems services. *Philosophical Transactions of the Royal Society B*, *370*, 20130273. doi: 10.1098/rstb.2013.0273

Sallée, J., Speer, K., & Morrow, R. (2008). Response of the antarctic circumpolar current to atmospheric variability. *Journal of Climate*, *21*(12), 3020–3039.

Sarmiento, J. L., & Gruber, N. (2006). *Ocean biogeochemical dynamics.* Princeton University Press.

Scheffer, M., Carpenter, S., Foley, J. A., Folke, C., & Walker, B. (2001). Catastrophic shifts in ecosystems. *Nature*, *413*(6856), 591–596.

Sokolov, S., & Rintoul, S. R. (2009). Circumpolar structure and distribution of the antarctic circumpolar current fronts: 2. variability and relationship to sea surface height. *Journal of Geophysical Research: Oceans*, *114*(C11).

Stock, C. A., & Dunne, J. (2010). Controls on the ratio of mesozooplankton production to primary production in marine ecosystems. *Deep Sea Research Part I: Oceanographic Research Papers*, *57*(1), 95–112.

Stock, C. A., Dunne, J. P., & John, J. G. (2014a). Drivers of trophic amplification of ocean productivity trends in a changing climate. *Biogeosciences Discussions*, *11*(7).

Stock, C. A., Dunne, J. P., & John, J. G. (2014b). Global-scale carbon and energy flows through the marine planktonic food web: An analysis with a coupled physical–biological model. *Progress in Oceanography*, *120*, 1–28.

Stock, C. A., John, J. G., Rykaczewski, R. R., Asch, R. G., Cheung, W. W., Dunne, J. P., … Watson, R. A. (2017). Reconciling fisheries catch and ocean productivity. *Proceedings of the National Academy of Sciences*, *114*(8), E1441–E1449.

Taniguchi, D. A., Franks, P. J., & Poulin, F. J. (2014). Planktonic biomass size spectra: an emergent property of size-dependent physiological rates, food web dynamics, and nutrient regimes. *Marine Ecology Progress Series*, *514*, 13–33.

Thomas, M. K., Kremer, C. T., Klausmeier, C. A., & Litchman, E. (2012). A global pattern of thermal adaptation in marine phytoplankton. *Science*, *338*(6110), 1085–1088.

Tilman, D. (1982). *Resource competition and community structure.* Princeton university press.

Ward, B. A., Dutkiewicz, S., Jahn, O., & Follows, M. J. (2012). A size-structured food-web model for the global ocean. *Limnology and Oceanography*, *57*(6), 1877–1891.

JOURNAL OF GEOPHYSICAL RESEARCH

Supporting Information for "Marine ecosystem changepoints spread under ocean warming in an Earth System Model"

B. B. Cael[1], Charlotte Begouen Demeaux[1], Stephanie Henson[1], Charles A. Stock[2], Fernando González Taboada[2], Jasmin G. John[2], & Andrew D. Barton[3]

[1]National Oceanography Centre, Southampton, UK.

[2]NOAA/OAR/Geophysical Fluid Dynamics Laboratory, New Jersey, USA.

[3]Scripps Institution of Oceanography and Section of Efcology, Behavior and Evolution, University of California San Diego, La Jolla, CA, USA

Contents of this file

1. Table S1
2. Figures S1 to S14

---

time series	best-fitting model	ΔAIC	ΔBIC
$N(0,1)$	Constant Mean	-2.5	-7.7
$(2t-1)+N(0,1)$	Trend	-0.9	-8.7
$(2H(t-50)-1)+N(0,1)$	Mean Changepoint ($n=1$, $t=50$)	-42.7	-40.1
$(2t-1)+(2H(t-50)-1)+N(0,1)$	Trend Changepoint ($n=1$, $t=50$)	-20.7	-12.9

Table S1. Example showing that changepoint detection (or lack thereof) is robust to the superposition of a trend. Four timeseries are considered, with $t = 0 \ldots 100$: 1. a standard Gaussian random noise, 2. (1) with a linear trend moving from -1 when $t = 0$ to +1 when $t = 100$ superimposed (i.e. using the standard minimum signal-to-noise ratio of 2 from the time of emergence literature e.g. (Dutkiewicz et al., 2019)), 3. (1) with a step function moving from -1 when $t < 50$ to +1 when $t > 50$ (and zero when $t = 50$) is simperimposed, and 4. (1) with both the step function and the trend superimposed. A constant function, a trend, a mean changepoint function, and a trend changepoint function (i.e. statistical models 1-4 from the text) are fit to each time series; the difference in the Akaike and Bayesian Information Critera (ΔAIC and ΔBIC, which are smallest for the best-fitting model) are given for each best-fitting model versus the next-best model. In both of the cases with (without) a step-function, a model with (without) one changepoint at $t = 50$ is best-fitting, irrespective of whether or not the trend is included. Note that $n = 1$ and $t = 50$ are not chosen *a priori* and the ΔAIC and ΔBIC values do not change with repeated draws from $N(0, 1)$.

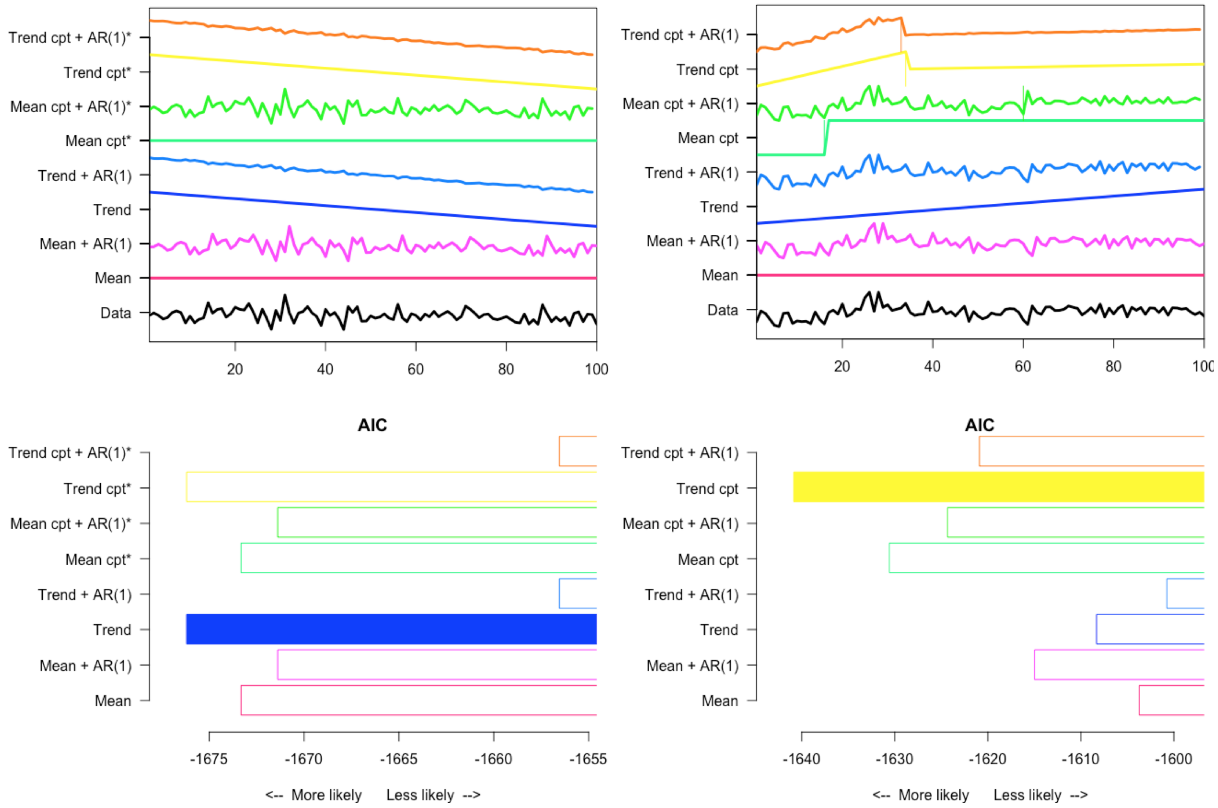

Figure S1. Example time series (both of nitrate in the 21st century (RCP8.5) simulation at 46°S) and standard output from the *EnvCpt* package. Left panels are at 178°W (no changepoint) and right panels are at 162°W (one changepoint). Top panels are fits of the different models and bottom panels are each model's Akaike Information Criterion (AIC) value, the lowest of which corresponds to the best fit.

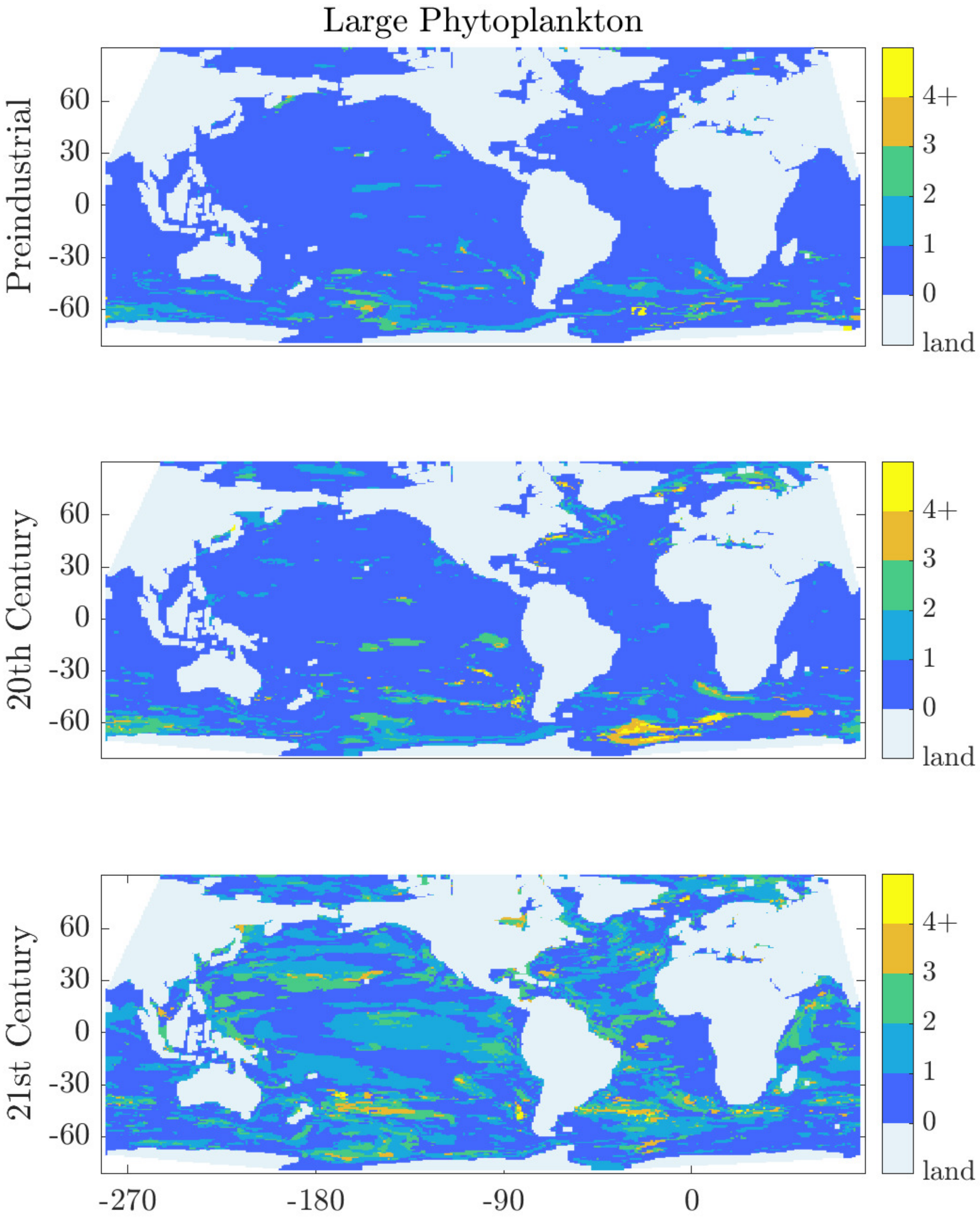

Figure S2. Maps of number of changepoints for each simulation for large phytoplankton.

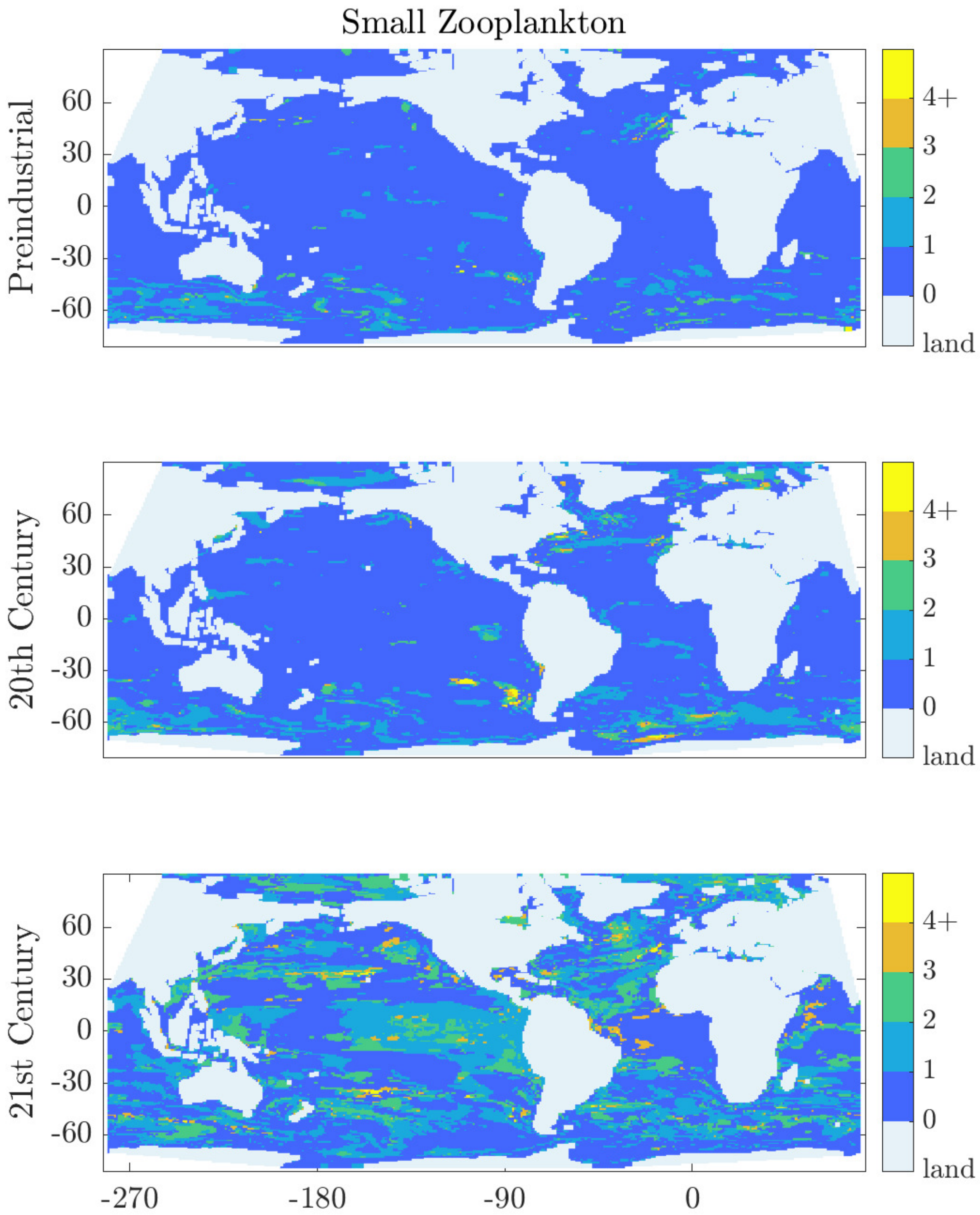

Figure S3. Maps of number of changepoints for each simulation for small zooplankton.

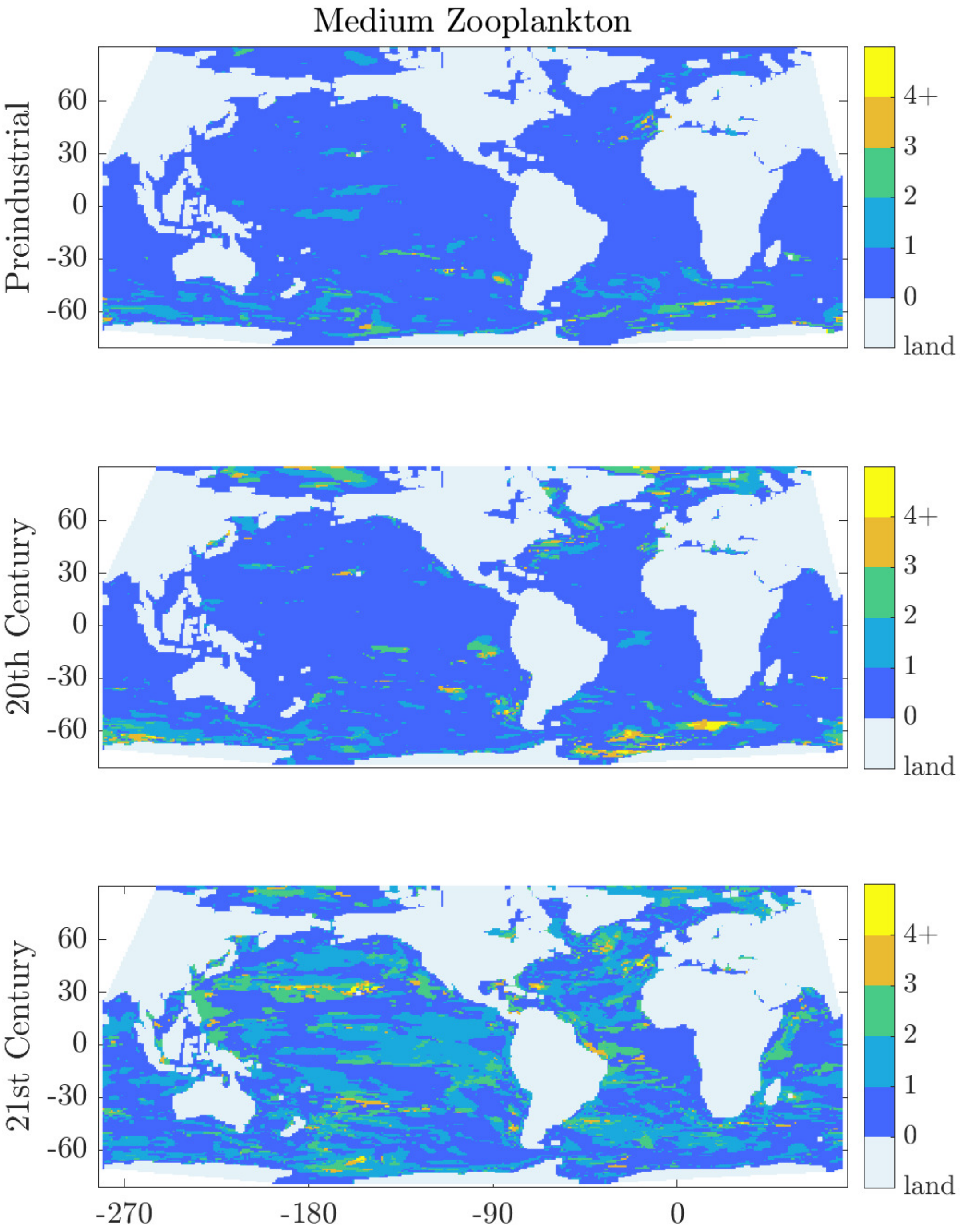
Medium Zooplankton
Preindustrial
20th Century
21st Century
60
30
0
-30
-60
-270
-180
-90
0
4+
3
2
1
0
land

Figure S4. Maps of number of changepoints for each simulation for medium zooplankton.

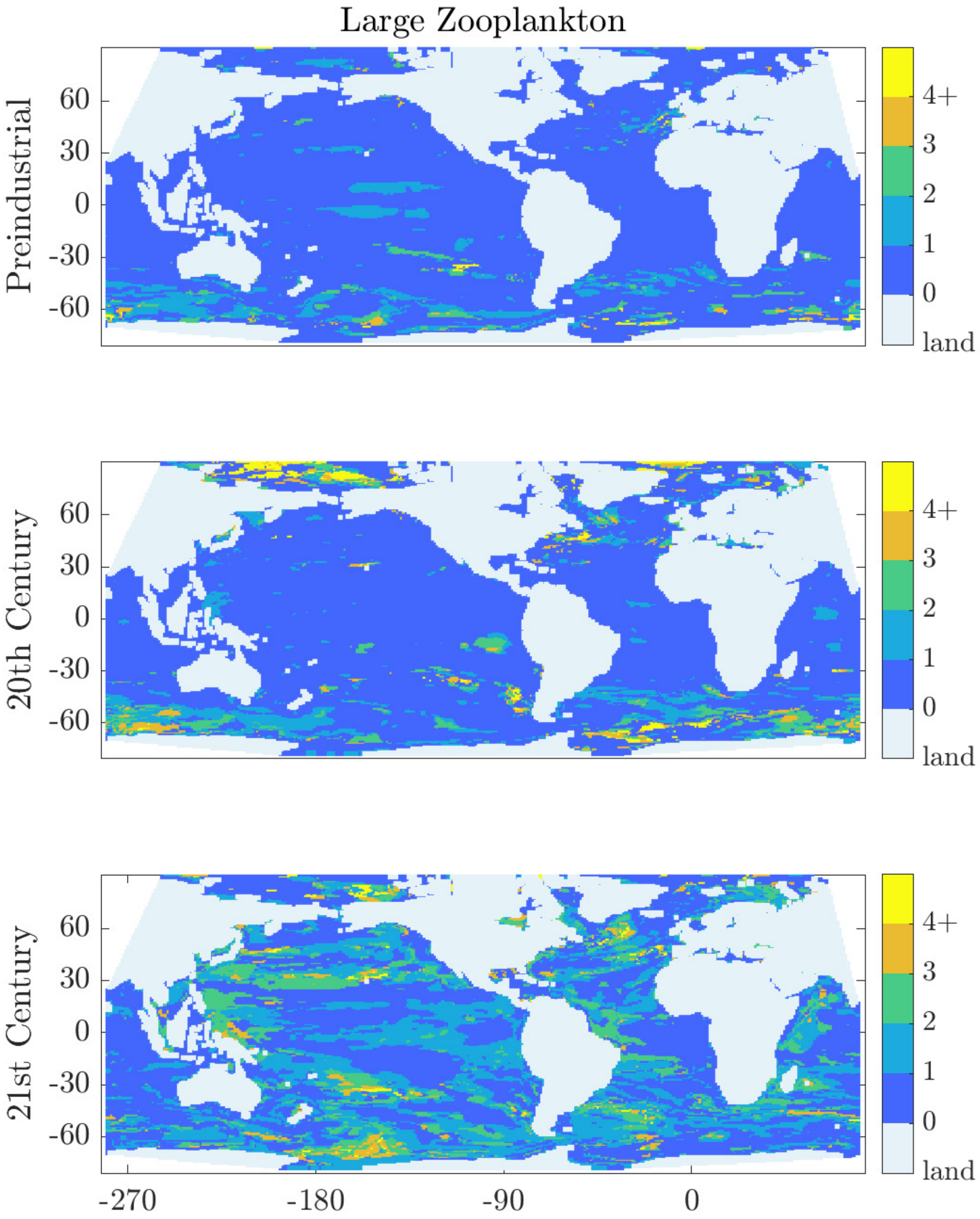

Figure S5. Maps of number of changepoints for each simulation for large zooplankton.

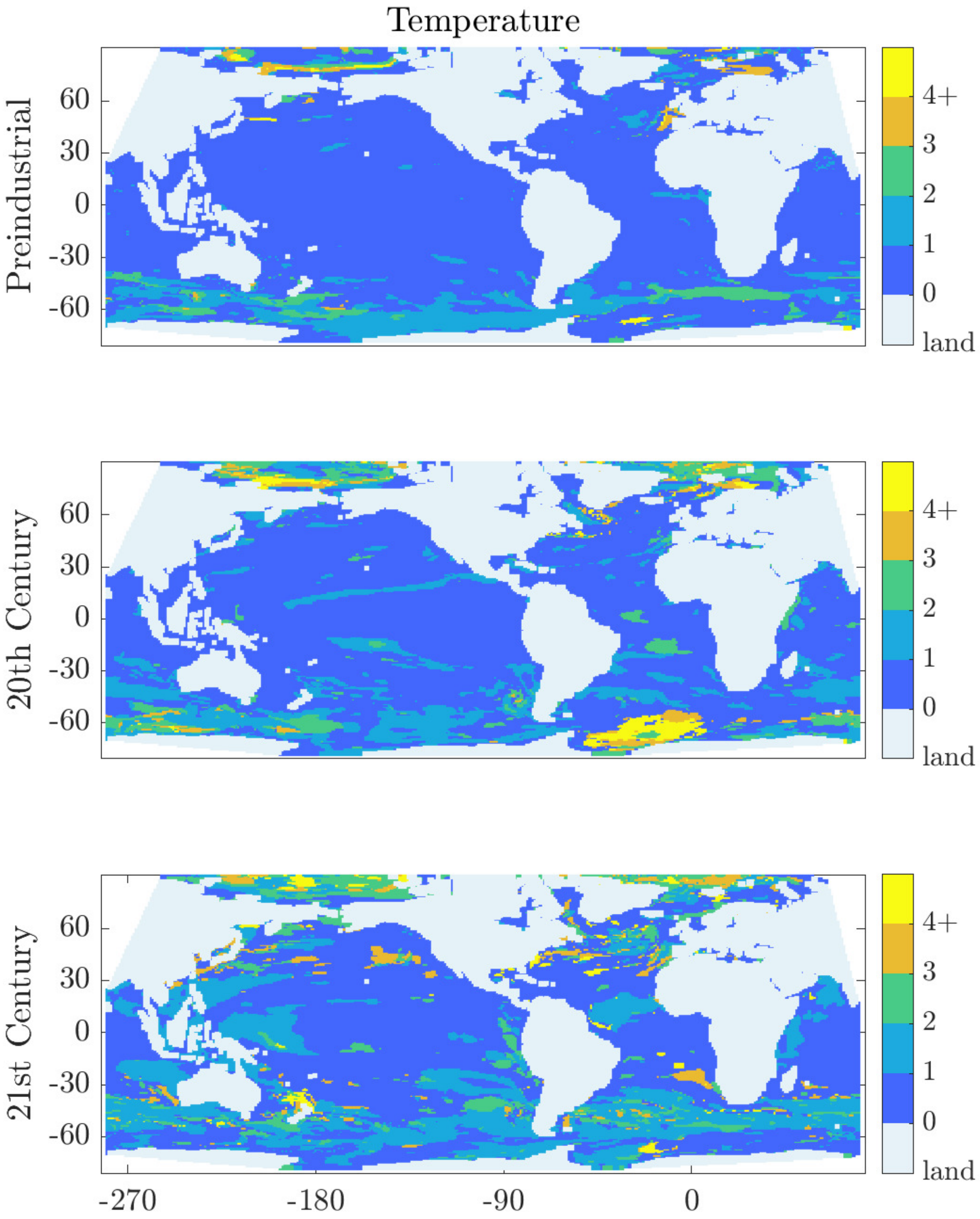

Figure S6. Maps of number of changepoints for each simulation for temperature.

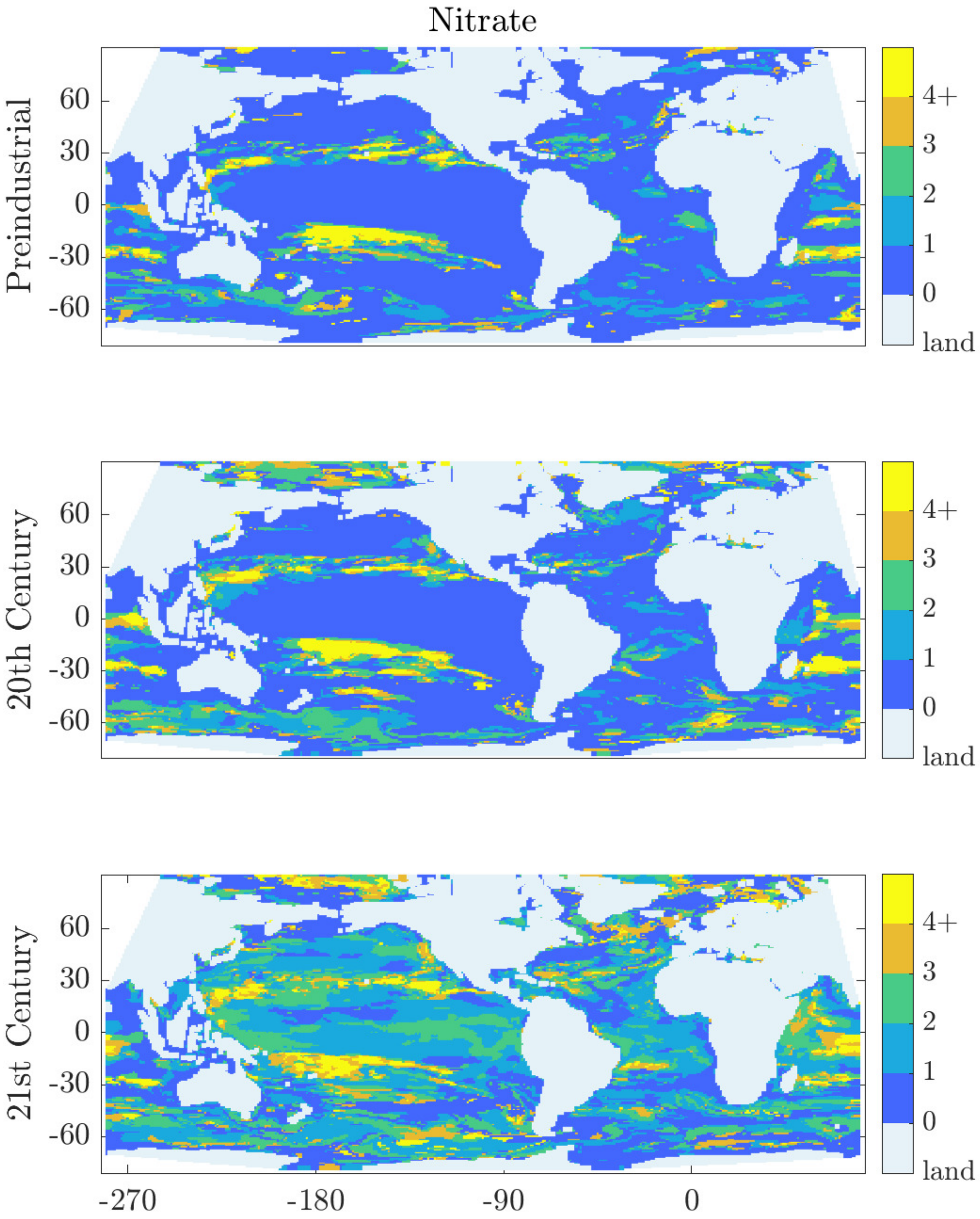

Figure S7. Maps of number of changepoints for each simulation for nitrate.

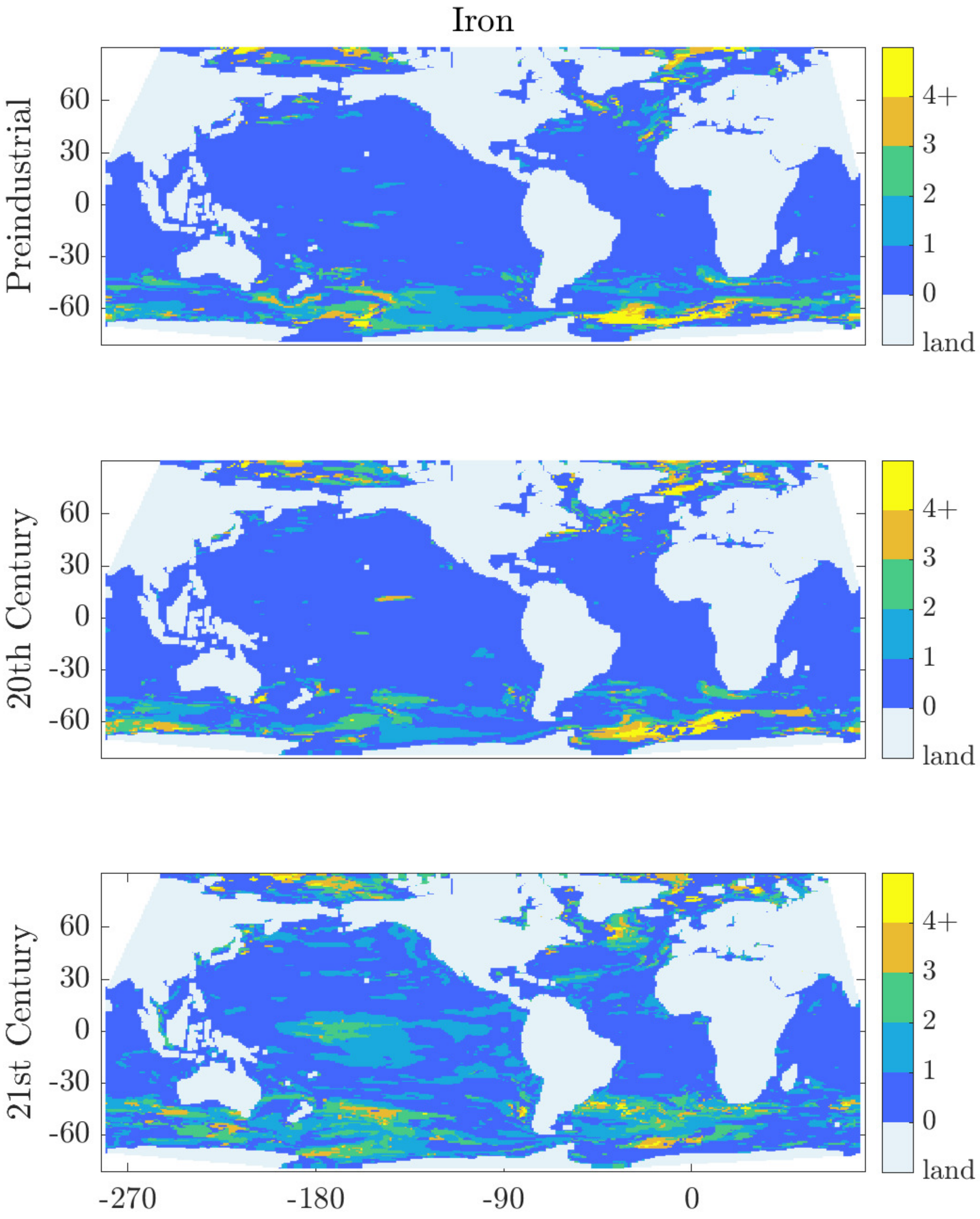

Figure S8. Maps of number of changepoints for each simulation for iron.

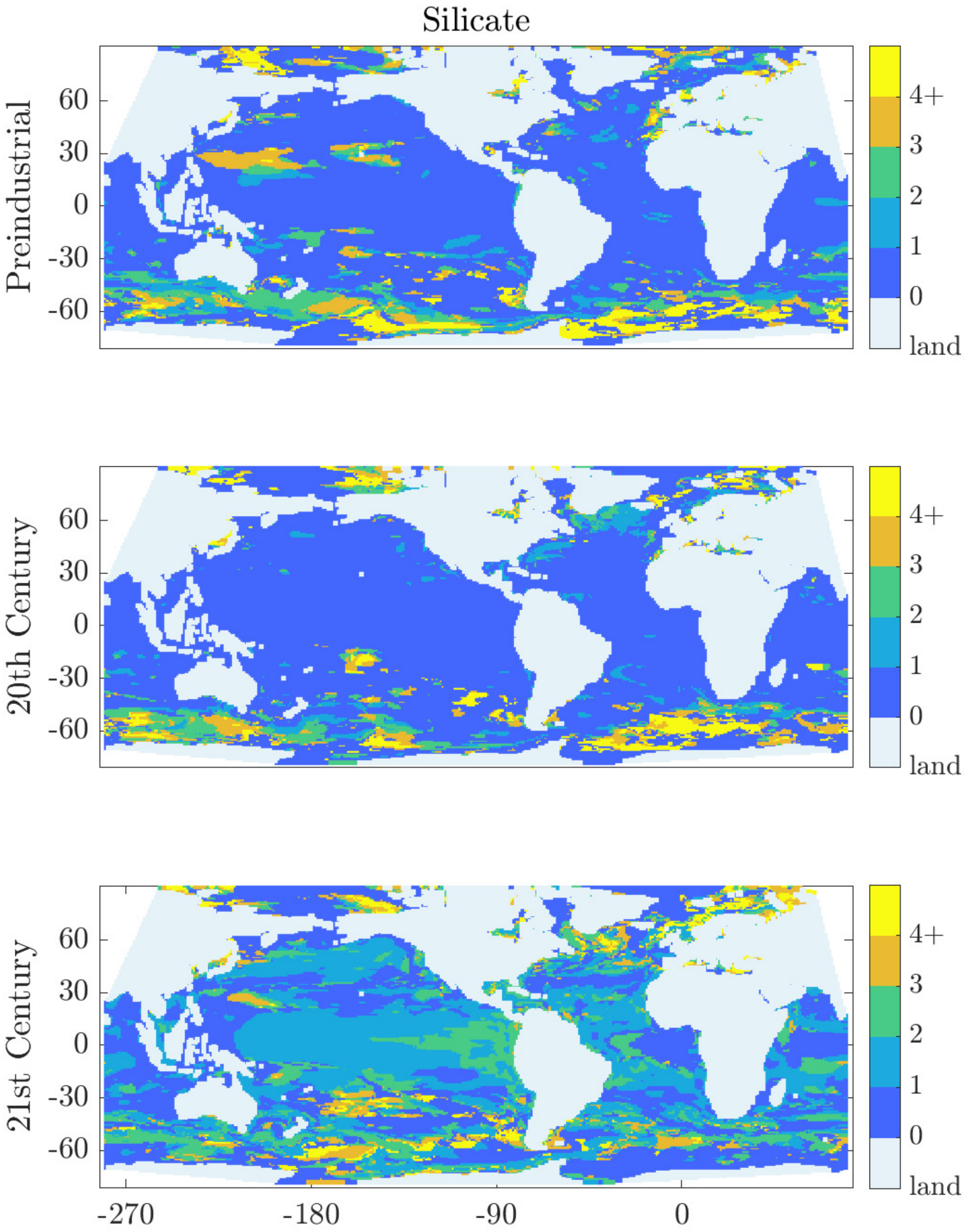

Figure S9. Maps of number of changepoints for each simulation for silicate.

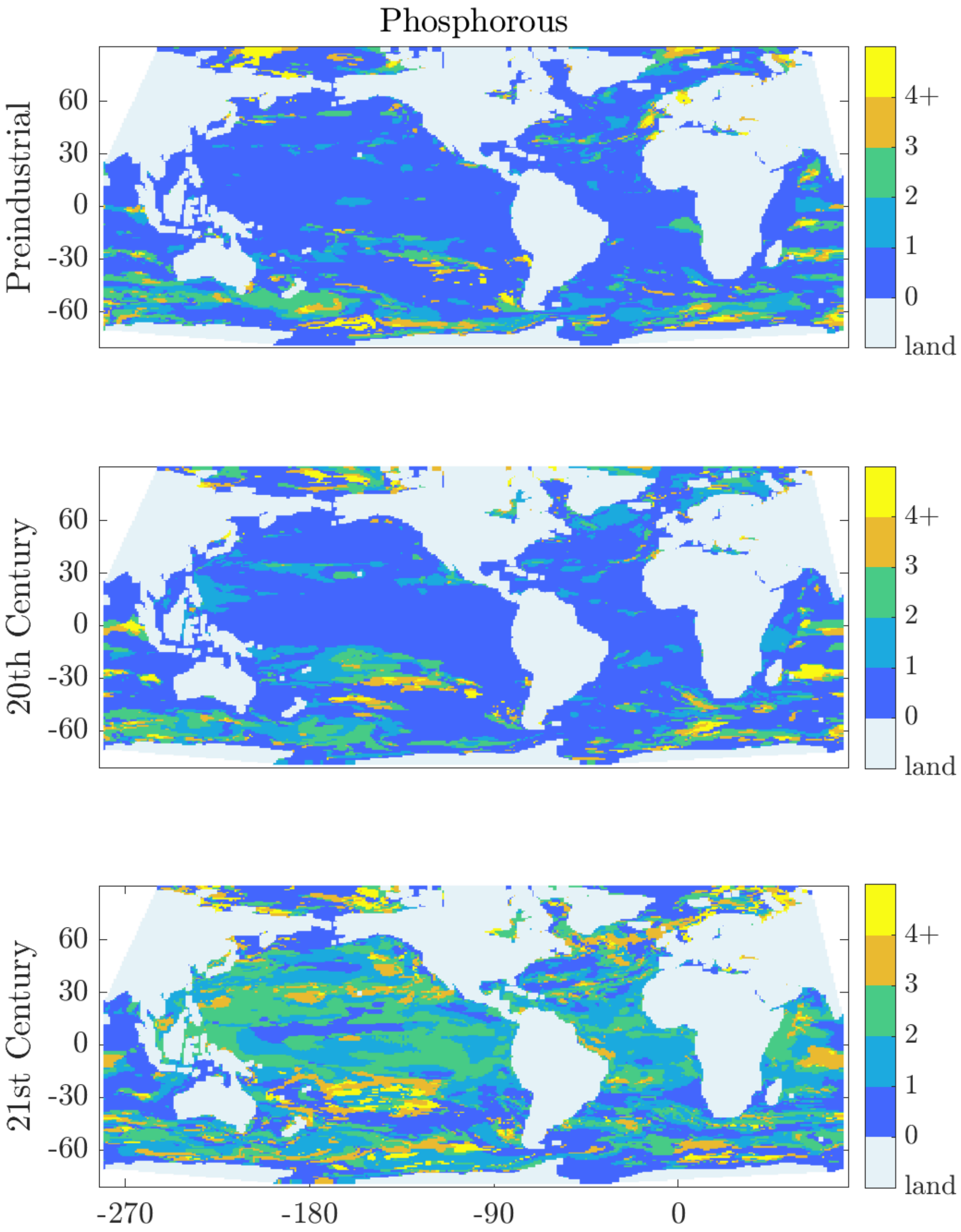

Figure S10. Maps of number of changepoints for each simulation for phosphate.

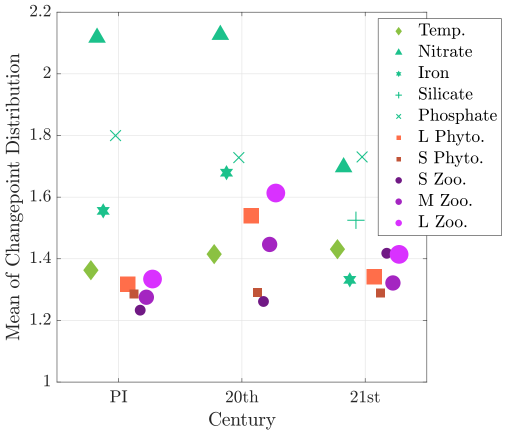

Figure S11. Mean of changepoint distribution (i.e. probability distribution of the number of changepoints per century for locations with one or more changepoints) for each variable and simulation. As most of the ocean has 0, 1, or 2 changepoints per century for all simulations and variables other than nitrate, the value of the mean is primarily reflective of the balance between the area having 1 vs. 2 changepoints per century.

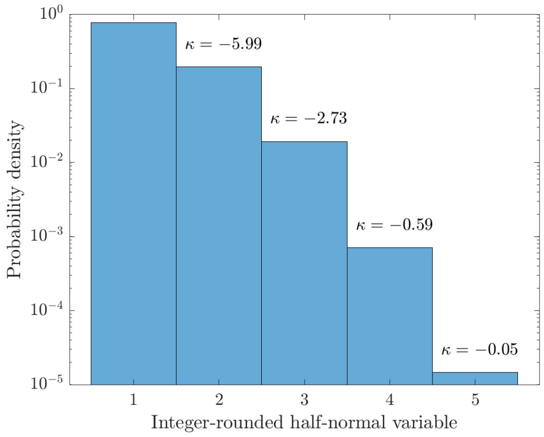

Figure S12. Distributions with different values of kurtosis κ, to illustrate how removing a distribution's tail reduces κ. By the definition of excess kurtosis we use here, a standard half-normal distribution rounded to integers and excluding zero values has a $\kappa = 0$; excluding values 5/4/3/2 and above produces lower κ values ($=-0.05/0.59/2.73/5.99$).

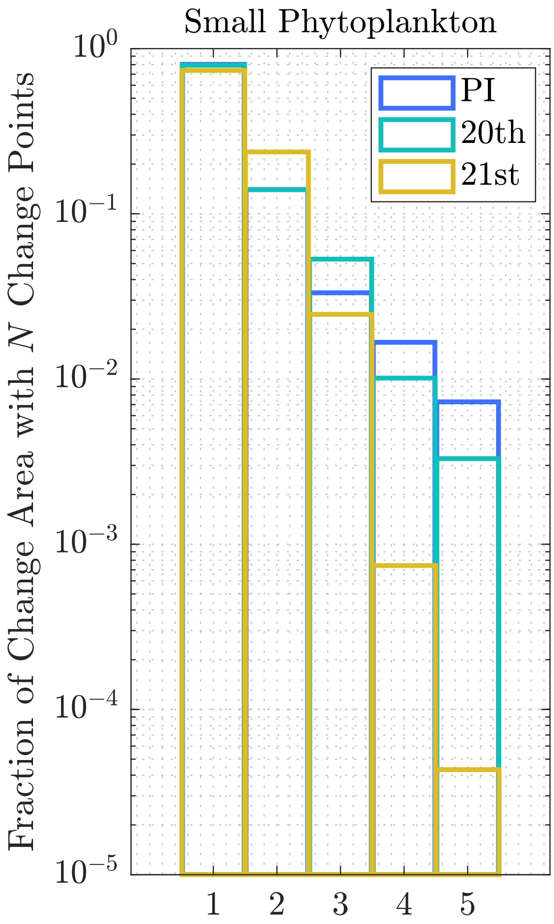

Figure S13. Distribution of the number of changepoints per unit area per century for small phytoplankton. y-axis is logarithmically spaced.

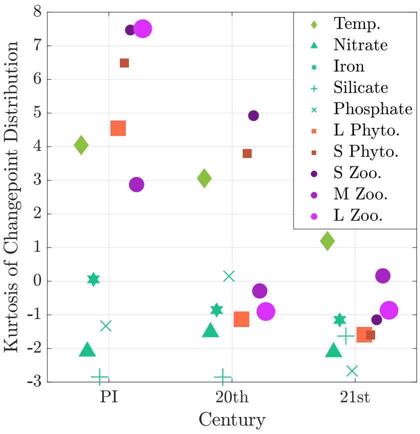

Figure S14. Same as Figure 9 but only for regions with changepoints for a given variable in the PI or 20th century.

References

Dutkiewicz, S., Hickman, A. E., Jahn, O., Henson, S., Beaulieu, C., & Monier, E. (2019). Ocean colour signature of climate change. *Nature communications*, *10*(1), 1–13.